Ocean Engineering 310 (2024) 118448

Contents lists available at ScienceDirect

Ocean Engineering

journal homepage: www.elsevier.com/locate/oceaneng

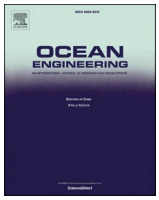

Research paper

The future of the Portuguese (SW Europe) most vulnerable coastal areas under climate change – Part II: Future extreme coastal flooding from downscaled bias corrected wave climate projections

Gil Lemos [a,*], Ivana Bosnic [b], Carlos Antunes [a], Michalis Vousdoukas [c], Lorenzo Mentaschi [d], Miguel Espírito Santo [a], Vanessa Ferreira [a], Pedro M.M. Soares [a]

[a] Universidade de Lisboa, Faculdade de Ciências, Instituto Dom Luiz, Lisboa, Portugal
[b] HAEDES, Portugal
[c] Department of Marine Sciences, University of the Aegean, University Hill, 81100, Mitilene, Greece
[d] University of Bologna: Bologna, Emilia-Romagna, Italy

ARTICLE INFO

Keywords:
Climate change
Coastal areas
Extreme coastal flooding
Overtopping
Projections

ABSTRACT

Episodic extreme coastal flooding is considered one of the most serious threats to the global coastlines, endangering infrastructure, ecosystems, and communities. The synchronized effects of extreme wave events, storm surges and astronomical tides are particularly worrying in the context of sea level rise (SLR), and a comprehensive understanding of their future dynamics remains challenging. In this study, an innovative approach for a vulnerability assessment of sandy low-lying coastal areas, based on dynamic ensemble projections is proposed. In the current Part II study, the combined effects of future projected SLR, tides, storm surges and wave action are investigated at five key-locations along the Portuguese coastline, considering projected digital terrain models, built upon the shoreline projections obtained in Part I. Future extreme total water levels are obtained through a probabilistic approach, and extreme wave events are defined considering high wave energy thresholds in a changing climate. Overall, extreme coastal flooding is projected across several urbanized sections along the Portuguese coastline, especially in areas without artificial protection infrastructures. Dune erosion is expected along the sandy stretches, reducing the natural protection against extreme coastal events up to 13.3%, and promoting widespread overtopping, leaving populations more exposed. Future projections reveal the episodic flooding of up to 1.47 km^2 of land along the 14 km of analyzed coastline, threatening households and commercial hubs, besides services and communication routes. As physical and human losses may increase substantially in the future, our results call for the implementation of adequate coastal management and adaptation plans, strategically defined to withstand changes until 2100 and beyond.

1. Introduction

Climate change represents an existential threat to coastal areas worldwide (Ranasinghe, 2016), with potentially dire consequences for natural ecosystems, coastal communities, cities, and relevant infrastructures. The global coastlines have long been serving as vital hubs of economic activity, transportation, recreation, and cultural heritage (IPCC et al., 2022; Hallegatte et al., 2013; Hinkel et al., 2014; Kulp and Strauss, 2020; Feyen et al., 2020; Vousdoukas et al., 2020), often developing faster than inland regions due to their unique and desirable attributes and location, making them increasingly vulnerable to climate change impacts (Jones and O'Neill, 2016). Although the focus of the public and decision-makers tends to be mainly on the changes in mean sea levels, future episodic extreme coastal flooding resulting from severe weather synchronized with wave action and high tides in the context of rising sea levels, is expected to further endanger coastal communities (Storlazzi et al., 2018; Camelo et al., 2020; Senechal et al., 2011). Such a threat calls for comprehensive adaptation and impact mitigation strategies to safeguard coastal areas, based on reliable, long-term coastal vulnerability assessments.

Coastal management is becoming increasingly relevant in the context of climate change (IPCC et al., 2022; Toimil et al., 2020;

* Corresponding author.
E-mail address: grlemos@fc.ul.pt (G. Lemos).

https://doi.org/10.1016/j.oceaneng.2024.118448
Received 24 December 2023; Received in revised form 2 June 2024; Accepted 7 June 2024
Available online 9 July 2024

Vousdoukas et al., 2017, 2018), as recent studies indicate significant projected changes not only in the mean sea levels (*e.g.*, Horton et al; Hsiao et al., 2022), but also in storm surges (*e.g.*, Marcos et al., 2011; Little et al., 2015), waves (*e.g.*, Hemer et al., 2013; Semedo et al., 2013; Morim et al., 2018, 2019; Lemos et al., 2019, 2020b, 2021b), as well as in tropical (Peduzzi et al., 2012; Woodruff et al., 2013; Chen et al., 2019; Hsiao et al., 2020; Knutson and Coauthors, 2020; Garner et al., 2017) and extratropical (*e.g.*, Bengtsson et al., 2009; Catto et al., 2011; Priestley and Catto, 2022) cyclonic activity. These changes are expected to enhance coastal flood risk worldwide (Vitousek et al., 2017; Wahl et al., 2017; Rasmussen et al., 2018), enhancing the role of adaptation and impact management strategies. In Portugal, the National Roadmap for Adaptation XXI – Portuguese Territorial Climate Change Vulnerability Assessment for XXI Century (RNA2100) project is currently underway, attempting to coherently characterize, for the first time, the climate change physical and socioeconomic impacts on the Portuguese most vulnerable domains (Lima et al., 2023a, 2023b; Soares et al., 2022a; Soares et al., 2023a,b; Soares and Lima, 2022; Bento et al., 2023; Cardoso et al., 2023).

Coastal flooding is a relatively-well understood and widely modelled consequence of increasing total water levels (TWLs), which combine sea level rise (SLR), astronomical tides, storm surges and waves (wave set-up and run-up). Some of the most pressing challenges to coastal flood modelling include coherent approaches to obtain and assess total water level (TWL) components in order to produce adequate (and accurate) results. While the probabilistic combination of the TWL components should be considered the methodology of choice, the deterministic approach of combining all TWL components is still common. Furthermore, when dealing with wave climate simulations and projections, the additional efforts required to account for the waves' interaction with bathymetry near the coast are usually neglected. In fact, coherent and comprehensive methodologies combining SLR with tides, storm surges and waves are scarce (Toimil et al., 2020; Vousdoukas et al., 2017). Despite some exceptions (Lin et al., 2016; Vousdoukas et al., 2016; Arns et al., 2020; Garner et al., 2017; Sayol and Marcos, 2018; Tebaldi et al., 2023), most studies focus uniquely on SLR, neglecting or considering the remaining variables stationary. Nevertheless, the combined impact of storm surges and extreme wave conditions, especially when synchronized with high tides, may produce variations in the TWLs greater than SLR, of up to a couple meters (Vousdoukas et al., 2017; Kirezci et al., 2020).

Despite the multivariate nature of coastal flooding and its drivers, the behavior of their individual components is not linear, and often not synchronized (Idier et al., 2019; Arns et al., 2020; Camus et al., 2021). Uncertainties also increase rapidly with each additional variable (Toimil et al., 2021). Therefore, even in dynamic modelling efforts, probabilistic approaches must be considered, rather than a simple addition of variables (*e.g.*, Arns et al., 2020; Leijala et al., 2018; Jevrejeva et al., 2019; Liu et al., 2020; Gori and Lin, 2022). Such approach incorporates uncertainties and variability associated with climate change, oceanographic processes, digital terrain models (DTMs) and vertical datums (Marcy et al., 2011; Antunes et al., 2019). This allows the consideration of non-synchronized events, for a more comprehensive range estimate of possible outcomes (Baldassarre et al., 2010; Thompson and Frazier, 2014), in the potential future vulnerability and risk assessments. Additionally, probabilistic methods to determine the projected TWLs can incorporate local effects of combined extreme events, namely related to storm surges and waves, which can have disproportionate impacts on coastal flooding.

Within the context of the RNA2100, Lemos et al., 2024a (Part I) presented, for the first time, consistent future shoreline evolution projections for five key-locations along the Portuguese coastline. These were selected due to their socio-economic relevance and widespread available field data, as well as their increased vulnerability to coastal flooding from historical extreme events. From Part I, extensive sedimentary deficits were identified, and shoreline retreat was shown to be expected, driven mainly by SLR. To complete a comprehensive assessment, from future shoreline evolution to extreme coastal flooding is, two parts as companion papers were needed. Here, in Part II, the main goal lies in assessing the physical impacts of future projected extreme coastal flooding on the five highly vulnerable key-locations, using the XBeach numerical model (Roelvink et al., 2009). This endeavour, conducted for the first time in a consistent manner for the Portuguese coastline, is based on three Coupled Model Intercomparison Project phase 5 (CMIP5) multi-model ensembles of SLR, storm surge levels (SSLs) and nearshore bias corrected wave climate projections towards the end of the 21st century, under the Radiative Concentration Pathways (RCPs) 4.5 and 8.5 (Riahi et al., 2011). The projected shorelines, obtained in Part I, are used to drive an innovative methodology to modify the reference DTMs into "new" future expected 3-dimensional coastal configurations for each key-location, to assess the extension of future extreme coastal flooding. Probabilistic TWL projections are built, based on the work of Antunes and Lemos (2024; *under review*), through the components' probabilistic combination based on their cumulative density functions (CDFs), and ensemble-based nearshore extreme wave events are characterized, based on their energy content. Finally, the ensemble-based projections of flooded areas are determined using the XBeach model, highlighting the effects of changing extreme water levels on coastal urbanized zones. The overall assessment, carried out in Part I and Part II, ultimately aims at providing the baseline results to allow the translation of the local dynamic modelling efforts into a national-scale assessment, through a composed coastal vulnerability index, enabling the identification of the potential risk zones well beyond the five key-locations analyzed here.

This article is organized as follows: in section 2, the study areas are identified, the datasets are presented, and the methodology of each subtask is explained. The results are described in section 3. In the context of the results, in section 4, a discussion is offered, along with a review of the current adaptation policies in Portugal, and recommendations for the future. The main conclusions drawn from Part II are also presented in section 4.

2. Data and methods

2.1. Study areas

Five specific key-locations were selected along the Portuguese coastline, considering their increased vulnerability to climate change and overall proneness to coastal hazards, as well as the existence of widespread field and reference datasets. Enhanced erosive trends and imminent overtopping and coastal flooding, together with the proximity of population centres to the coast were criteria to the selection of the key-locations: Ofir, Costa Nova, Cova Gala, Costa da Caparica and Praia de Faro (Fig. SM1 in the Supplementary Material - SM).

Ofir is located in the northwestern coast of Portugal, in a particularly vulnerable area due to intensive human occupation along the coastal fringe. Historical erosion trends of up to −4 m/year have been observed (Ponte Lira et al., 2016). Future shoreline projections in Lemos et al. (2024a) – henceforth "LP1" – depicted a consistent retreat, peaking at 120 m by 2100 under the RCP8.5 scenario. The 3-km coastal stretch is projected to lose up to 0.188 km^2 of dry land.

Costa Nova is a sector of the central Portuguese western coast, located South of Ria de Aveiro mouth. Historical erosive trends are larger in this sector, reaching −7 m/year (Ponte Lira et al., 2016; Pinto et al., 2022). Projected shoreline retreat of up to 210 m, together with a reduction in dry land area of 0.197 km^2 along this 3-km stretch is expected by 2100 (RCP8.5).

Cova Gala, located in the central Portuguese western coast, South of Figueira da Foz, shows increasing historical erosion trends (Oliveira and Brito, 2015; Nunes and Cordeiro, 2013), locally reaching −4 m/year (Pinto et al., 2022). LP1 revealed projected shoreline retreat of up to 150 m by 2100 (RCP8.5), and an overall decrease in dry land area of

0.118 km^2, along this nearly 2-km-long coastal stretch.

Costa da Caparica is a densely occupied urban area and touristic resort located South of the Tagus River mouth, benefiting from its proximity to Lisbon. Major coastal planning efforts have been put in place over time to mitigate and adapt to the local enhanced coastal erosion trends (of up to −4 m/year; Pinto et al., 2007). Shoreline projections indicate retreat of up to 300 m, and a loss of 0.175 km^2 of dry land by 2100, under RCP8.5 over the 4-km stretch (LP1).

Praia de Faro, in the Ria Formosa natural park in the Algarve region, close to the city of Faro, is home to a small community of fishermen and used as a recreational area for tourists and locals. It is undergoing long-term erosion driven by changes in the sea level, storms and human interventions (historically up to −2 m/year). Projected shoreline retreat is not projected to exceed 80 m by 2100 (RCP8.5; LP1), but it is consistent along the 2-km-long coastal stretch, leading to a reduction in dry land area of up to 0.119 km^2.

2.2. GCM-Driven wave climate projections and SLR

A few studies in recent scientific literature dealt with the problematic of future extreme sea levels along the European coasts. Vousdoukas et al. (2017) presented a dataset of extreme storm surge levels (SSLs) and wave climate projections forced by 6 CMIP5 GCMs for the RCP4.5 and RCP8.5 scenarios, with increased horizontal resolution along the European (and therefore Portuguese) coastlines. These ensembles, forced by the same GCMs and produced for the same domains, using the same resolution, present a high degree of consistency, which is rare, especially considering that such GCMs are also included in the SLR projections (described below).

Regarding wave climate simulations and projections, the 6-member ensemble originally described in Vousdoukas et al. (2017) and Mentaschi et al. (2017), and employed in LP1, is also considered here. The spectral wave model WaveWatchIII (WW3; Tolman, 2002) was set-up using the ST4 parameterization (Ardhuin et al., 2010), generating simulations and projections covering the 1971–2100 period, with a horizontal resolution of 0.5° for southwestern Europe. The wave parameters considered here include the significant wave height (H_S), the peak wave period (T_p) and the mean wave direction (*MWD*). Further details can be found in Table SM1.

The SLR projections used here were obtained from CMIP5 GCMs outputs, following Church et al. (2013). The complete SLR dataset includes projections from 21 GCMs for the RCP4.5 and RCP8.5 future scenarios. The mean SLR projections are extracted from each ensemble, at closest grid-point to each key-location (Table SM2).

2.3. Tides

All tidal data are referred to the vertical reference used in hydrography, the chart datum, defined in Portugal as the lowest low-tide (minimum low water) observed during a period longer than 19 years (the Moon's 18.6-year nodal period; Haigh et al., 2011; Pugh et al., 2014; Wahl and Chambers, 2015), plus an additional safety margin (one foot). For all Portuguese tide ports, the chart datum is 2.00 m below the national vertical reference, the 1938 Cascais Vertical Datum (CASCAIS1938), except for the Tagus River estuary, where the chart datum is 2.08 m below the mean sea level. These values were removed from the hydrographic tide heights to obtain the tide elevations, which correspond to the tide orthometric heights relative to CASCAIS1938 datum.

To generate future tidal projections, numerical modelling was employed, based on harmonic analysis, considering long time-series of the national tide gauge network data (Antunes, 2007). Through the harmonic tide models, a long-term-based CDF (30 years) was generated for each key-location.

2.4. Storm surges

Storm surge is the abnormal water level above (or below) the predicted astronomical tides, caused by meteorological forcing, through the joint effect of low atmospheric pressure and persistent wind friction on the sea surface. In Portugal, according to Vieira et al. (2012), based on the analysis of tide gauge data series from 1960 to 2010, maximum storm surge values between 0.80 m and 1.10 m were obtained for long return periods (RPs), of 100 years or more. Higher-magnitude SSLs can nevertheless occur under very strong onshore wind and very low air pressure conditions or additional wave set-up effects. For the local scale assessment across the five key-locations, the SSLs were used to compute the TWLs through the probabilistic combination with SLR projections and tides. The SSL projections were generated using the Delft3D-FLOW, designed to simulate wave propagation, currents, sediment transport, morphological developments and water quality aspects in coastal, river and estuarine areas (Roelvink and Van Banning, 1994). Additional details in Vousdoukas et al. (2017) and LP1.

For each future 30-year climatological period and scenario, extreme SSL events corresponding to the 100-year RP were selected using a Generalized Extreme Value (GEV) distribution and integrated the future projections of extreme TWL. Note that the original SSL simulations and projections (Vousdoukas et al., 2017) were corrected considering the biases found in comparison with the measurements from the Cascais tide gauge during the historical climate, using a simple "delta" method (Hay et al., 2000; Lemos et al., 2020a), consisting of adjusting the SSL simulated distributions by the "delta" difference between the 50th percentile of the Cascais tide gauge observations and the originally simulated SSL values (Figs. SM2 to SM6 and Table SM3). The same correction terms were applied to all future SSL projections, assuming that the biases remain stationary throughout the entire simulated period (Maraun, 2016; Rocheta et al., 2017).

2.5. Reference datasets

The ERA5 reanalysis (Hersbach et al., 2020), produced using the ECMWF Integrated Forecast System (IFS) Cy41r2 (ECMWF, 2016), provides a detailed record of the global atmosphere, land surface and ocean waves from 1940 onwards, being updated in almost real-time. The ERA5 global grid has a horizontal resolution of 0.25° (31 km) for the atmosphere and 0.36° (40 km) for the waves, and output time resolution of 1 hour. Wave data from the ERA5, comprising H_S, mean wave period (T_m), T_p and *MWD*, are used as a long-term continuous reference dataset.

Despite using advanced assimilation methods based on *in-situ* observations and satellite altimetry measurements, the ERA5 is not able to capture local phenomena as accurately as the buoys. Therefore, to promote a more correct representation of local features, such as changes in *MWD* driven by nearshore bathymetry, *in-situ* wave observations were used to correct the ERA5, propagated from the original offshore location towards the *in-situ* location, using a quantile mapping bias correction methodology (LP1). Five buoys were considered, the nearest to each key-location. The geographical location and period covered by each buoy can be found in Table SM4. Then, the corrected ERA5 was propagated again, from the buoy location to nearshore, between 10 m and 20 m depth, where it was used to correct the (also propagated nearshore) wave climate simulations and projections (section 2.2.).

2.6. Methodology

The employed methodology focuses on obtention of high-resolution results, based on consistent forcing, as previously described in LP1. Further details regarding the datasets, the wave propagation, bias correction methods and shoreline evolution projections can be found in Part I. In essence, the methodology for the entire dynamic modelling approach can be summarized in four steps.

1) Propagation of the 6-member GCM-driven ensemble of wave climate simulations and projections to nearshore, using the SWAN wave model (Booij et al., 1999; adjusting the outputs to the reference datasets using bias correction methods from Lemos et al., 2020a, 2020b).
2) Employment of the ShorelineS model to obtain local high-resolution shoreline projections.
3) The impact of the extreme wave events and TWLs onshore is now assessed (in Part II), using the XBeach hydrodynamic model, on the future projected three-dimensional coastal configurations of each of the five key-locations, represented by the modified DTMs.
4) Finally, extreme coastal flooding projections are obtained, by the end of each future climatological period (2041–2070 and 2071–2100), and their impacts are analyzed.

Fig. 1 depicts the methodological framework of the entire assessment, from the original datasets to the final extreme coastal flooding projections, conducted at each key-location.

2.6.1. Future projected DTMs

The shoreline evolution projections presented in LP1 provided a baseline reference to build the three-dimensional structure of the projected DTMs, at each key-location. The new coastal configuration is crucial for an accurate assessment of the extreme TWL and wave impacts on the coastal environment, infrastructures and communities.

The projected shorelines were merged to an equilibrium coastal profile, resulting in a new coastal topo-bathymetric configuration, generated by the innovative Parametric Coastal Retreat (PaCR) algorithm, based on the modified Bruun rule (Rosati et al., 2013), and applied in a one-dimensional approach to each individual transverse topo-bathymetric profile, with a spatial resolution of 50 m alongshore and 2 m cross-shore. Figs. SM8 to SM12 in the SM depict the location of the profiles used to generate the future projected DTMs.

A semi-automatic process, run in a Geographic Information System environment, was developed to apply the PaCR semi-empirical approach for coastal retreat. The PaCR algorithm, developed by Antunes (2017), applies an elasticity function ($E(X)$ in Eq. (2)) to a beach profile, scaled

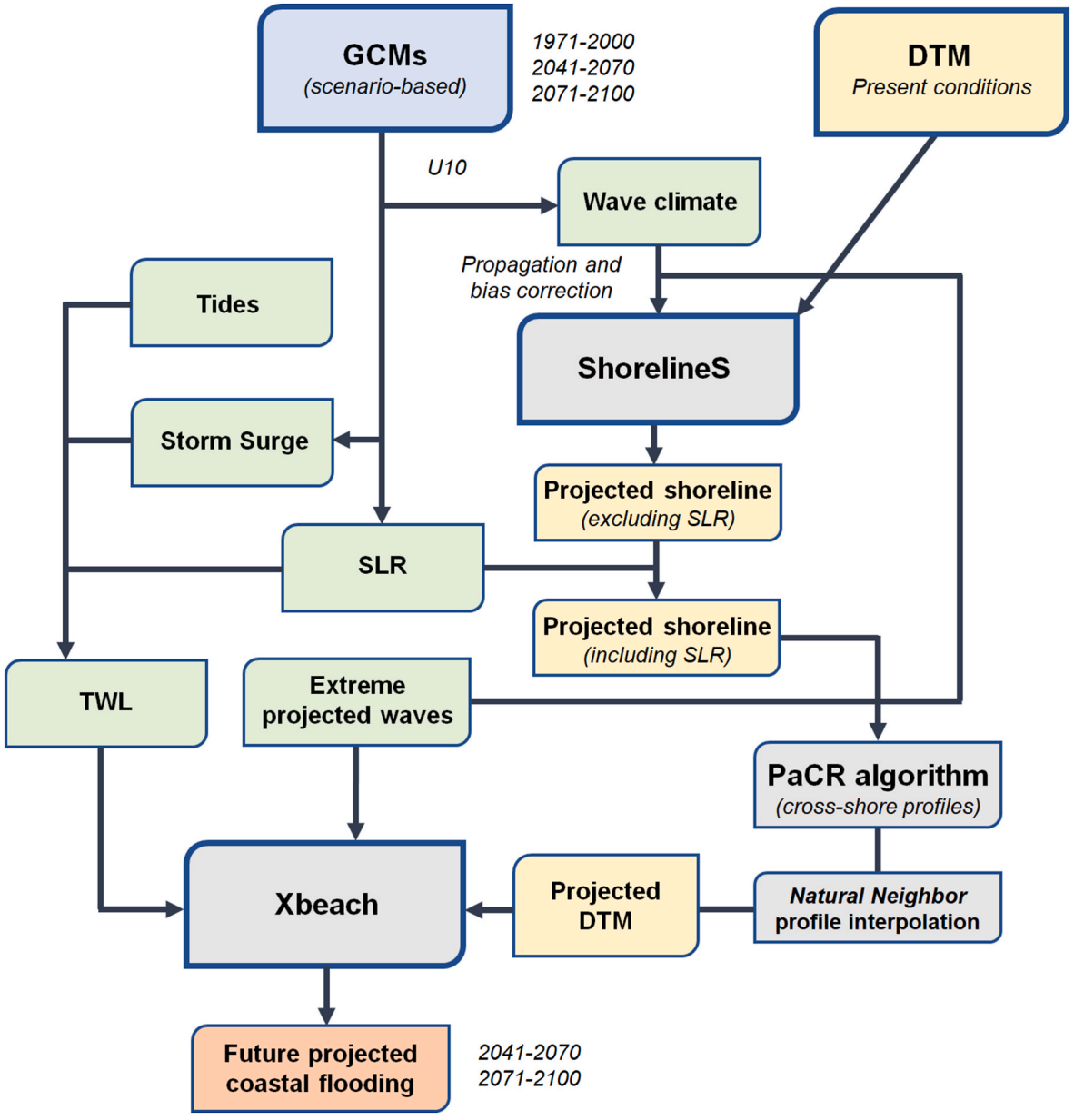

Fig. 1. Methodological framework of the dynamic modelling assessment in both Part I and Part II of the study, conducted for each future period and climate change scenario.

to the shoreline retreat (R). Such an elasticity function represents a binary force (torque), to reproduce both the sediment flux oceanward and landward, as in the modified Brunn rule principle. Eq. (1) and Fig. SM7 in the SM describe the modified Bruun rule, where Y_L represents the landward sediment transport, W^* the baseline from the closure profile depth to the maximum of the total run-up level (considering each 30-year climate period), and $B = B_0 + h^*$, with B_0 as the topographic height of the maximum TWL and h^* the closure depth of the topo-bathymetric profile. In Eq. (2), H corresponds to the orthometric height of both the original and the modified DTMs, at each X (cross-shore) coordinate, with origin at $H = 0$ m, being positive (negative) for positive (negative) H. The n-scaled elasticity function E is applied around X_{MLW}, which corresponds to the reference minimum low water (MLW) position, for the lowest recorded tide at the location. Finally, $E(X)$ corresponds to the modified X coordinate. The scale factor n is a parameter calibrated with historical shoreline retreat data. It depends on the erosion dynamics and shoreline response to erosion forcing factors. Along the Portuguese sandy coastlines, n ranges from 3 to 9, from low to high erosion dynamics environments, corresponding, for example, to the Faro and Costa da Caparica (specifically at São João da Caparica, in the northern top of the domain) key-locations, respectively. In a wider approach, if inland waters were to be considered, where SLR is the dominant forcing factor of coastal retreat, and lower or non-erosive process are present, smaller n scale factors would be more appropriate. Fig. SM13 summarizes the approach to obtain the future projected DTMs.

$$R = (W^* + Y_L) \bullet log\left(\frac{B}{B - SLR}\right) \tag{1}$$

$$E(X) = n \bullet R \bullet \frac{X - X_{MLW}}{W^*} \;\; \& \;\; H(X) = H(X) \bullet \left(1 - SLR^{2.0}\right), if \quad X > 0$$
$$E(X) = X \;\; \& \;\; H(X) = H(X) \bullet \left(1 - SLR^{2.7}\right), if \quad X < 0 \tag{2}$$

Before applying the PaCR algorithm, a coordinate system rotation transformation was conducted. The original DTM is defined in the cartographic coordinate system PT-TM06/ETRS89 (Portuguese Transverse Mercator of 2008 with the European Terrestrial Reference System, 1989), with three-dimensional coordinates (X, Y, H). From this DTM, for a coastal stretch of generally the same orientation, a set of cross-shore profiles spaced by 50 m are obtained. Each individual profile, with 2 m resolution, is transformed into a local coordinate system (X, H), where transformed X-coordinate corresponds to the transverse position relative to shoreline defined by the mean sea level ($H = 0$ m), or the profile

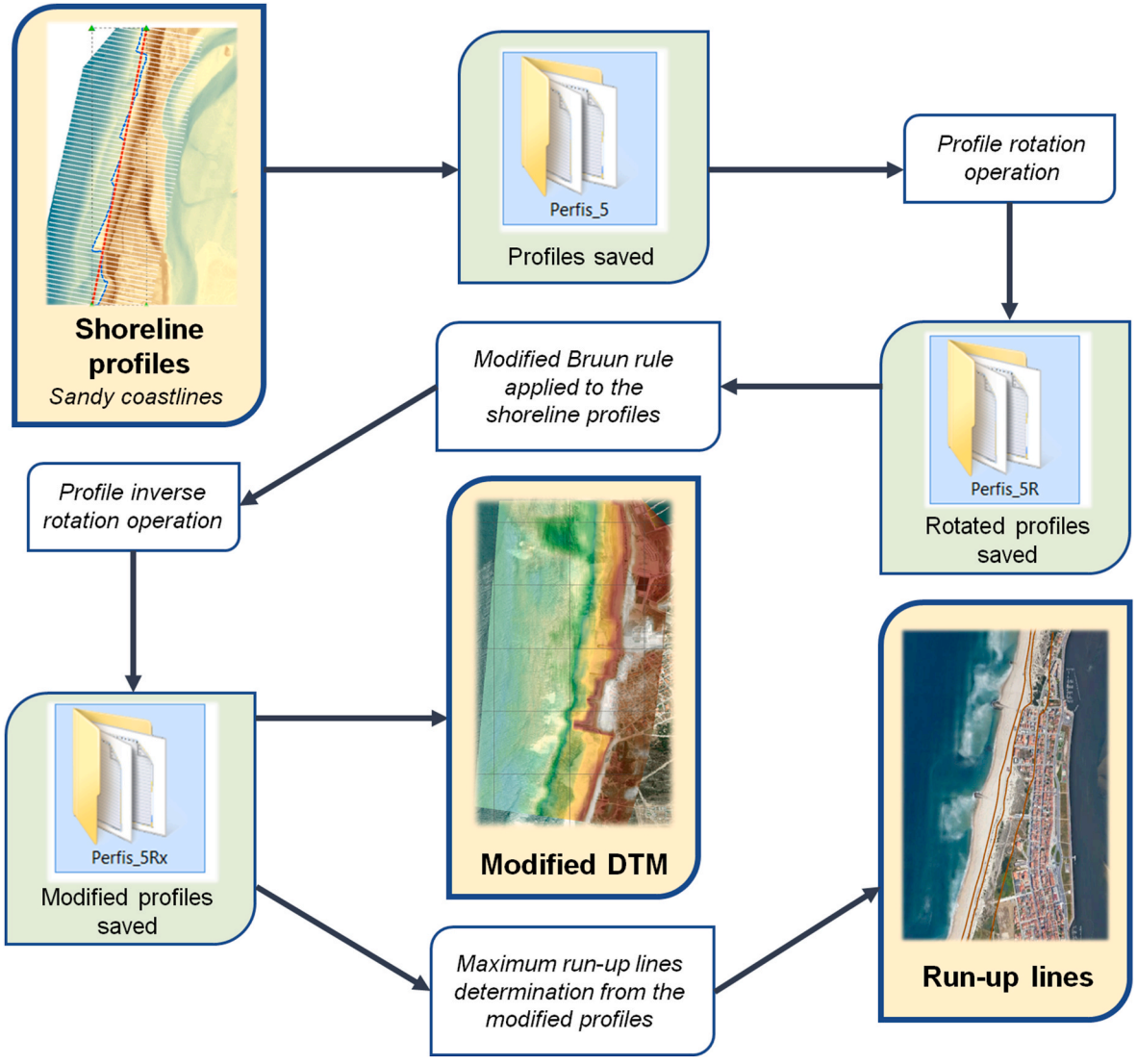

Fig. 2. Flowchart of the semi-empirical modelling approach to determine the coastal setback lines and build the future projected DTMs based on a semi-automatic supervised process run in Geographic Information System environment, for each key-location.

length component, and *H*-coordinate is the original orthometric height. After the PaCR algorithm is applied, the local coordinates, modified by the algorithm, are inversely transformed to the original cartographic coordinates, obtaining the modified DTM. After all topo-bathymetric profiles were modified accounting for SLR, two outputs can be derived, which are used in a later stage to produce the national-scale coastal vulnerability assessment:

1) The new retreated shoreline, based on the maximum wave run-up for a projected SLR, following Antunes (2014) and Antunes et al. (2019), considering the sum of the set-up and the incident run-up.
2) A modified DTM, built from the total profile dataset, consisting of a set of points, through spatial interpolation. This process is performed in a Geographic Information System software, by first building a TIN model, and then interpolating the grid points using the Natural Neighbor interpolation method (Figs. 1 and 2).

The resulting DTMs are used as forcing to the XBeach model, over which extreme coastal flooding projections are obtained.

2.6.2. Representative TWL projections and extreme waves

The last phase of the dynamic modelling across the five key-locations uses the XBeach model to project future coastal flooding conditions with high resolution (4 m cross-shore and 20 m alongshore), based on the projected DTMs supported by the shoreline projections of LP1. The forcing hydrodynamic conditions are composed of extreme TWLs (accounting for SLR, tides and SSs) and sea states (H_S, T_p and *MWD*). To reduce excessive computational costs, single events were used to define the forcing conditions, represented by one TWL and one value for each wave parameter.

Ensemble approaches are considered for both the TWL and waves, focusing on extreme events, which pose greater coastal threats. For the TWL, representative projections of the 25-year RP are used, based on Vousdoukas et al. (2017). The probabilistic determination of the TWL, through a Monte Carlo approach, assumes each component as a random variable, with a specific probabilistic density function (PDF). All components are considered as independent variables, and therefore, the joint probability of the TWL can be given by the probability product of the components (Eq. (3)):

$$P(TWL) = P(SLR)^{*}P(tide)^{*}P(SS). \quad (3)$$

Departing from the harmonic tide projections, random (non-synchronized) SS levels and SLR values are superimposed, extracted from the respective CDFs (ranging from 0.1% to 99.9% probability in 0.1% intervals), resulting in a large sample of TWL values for each future period ($\sim 2.6 \times 10^8$), from which a representative TWL PDFs can be computed. The complete sample allows the extraction of representative TWL RPs, avoiding a deterministic approach (*i.e.*, by simply adding the independent TWL components).

For wave action, three levels were selected, representative of the ensemble's uncertainty range. This process can be summarized in four steps.

1) To account for the multivariate wave conditions, an energy indicator was first computed, based on the formula for wave energy flux ($E = \left(\rho g^2 / 64\pi\right) T_m H_S^2$; Holthuijsen, 2007).
2) For each of the 6 ensemble members, the future projected event better corresponding to the 99th percentile of E was selected. In this approach, the T_p was used instead of the T_m, being T_p the peak period corresponding to the most energetic wave component in the wave spectrum.
3) The ensemble conditions corresponding to the lower and higher energy bounds, as well as the average for the 99th percentile of E, were selected.
4) Finally, the associated H_S, T_p and *MWD* were extracted.

Note that each of the three 99th percentile energy levels are not directly related to the extreme coastal flooding extent, considering that even lower energy extreme wave characteristics combined with a favorable *MWD* can lead to greater flooding than the most energetic ones, if the incoming *MWD* is unfavorable (*i.e.*, not perpendicular to the shoreline). Therefore, the three wave energy levels are henceforth named as "WAVES1" to "WAVES3", depicting the ensemble uncertainty range, and associated projected probability of occurrence (being "WAVES2" the most likely projection, *i.e.*, the average of the 99th percentile of E).

2.6.3. The XBeach model

The XBeach (Roelvink et al., 2009) was used to compute future projected extreme coastal flooding, based on projected DTMs and hydrodynamically forced by TWLs and nearshore extreme wave conditions. The XBeach was run under 2DH mode with absorbing-generating boundary conditions at the offshore forcing. The advanced default parameter values recommended by the developers were considered to run a wave-resolving non-hydrostatic model. Additionally, the formulations considered non-stationary shallow water equations and a pre-defined JONSWAP wave spectrum. Note that since the TWL was computed "offline" using a joint probability approach (section 2.6.2.) at each location and given the particular interest of the study on the extreme events, the XBeach was run considering extreme TWLs resulting from the probabilistic combination of extreme SSLs and tides (under a mean SLR). Extreme wave conditions were selected according to the nearshore total wave energy ("WAVES1" to "WAVES3"). All modelling domains were represented by regular grids with spatial-varying resolution (from 20 m offshore up to 3 m onshore). The landward expression of coastal flooding is finally given by the interception between the "water level" parameter and the DTM (run-up limit).

3. Results

3.1. Future shoreline projections and DTMs

In Part I, future shoreline evolution projections were presented for the five key locations along the Portuguese coastline. These considered the effects of continuous wave action (up to 2070 and 2100) and SLR (LP1). Consistent overall shoreline retreat was shown to be expected for all key-locations, mainly driven by SLR, whereas the shape of the shoreline was shown to be mostly affected by changes in the climatological wave characteristics, especially *MWD*, leading to northward beach rotation, especially in the northern and central western coastlines of Portugal Mainland. These new high-resolution shoreline projections were then used to drive the PaCR algorithm along the cross-shore profiles, allowing to modify the reference DTMs accounting for the projected changes in the shorelines.

Fig. 3 shows, for each key-location (each row), the reference (2018) and projected DTMs by 2070 and 2100, under the RCP4.5 and RCP8.5 scenarios. Figs. SM14 to SM38 in the SM detail each panel of Fig. 3. Fig. 4 highlights the projected changes in cross-section profiles at vulnerable sandy sections of each key-location. At Ofir (Fig. 3a–d), the reference DTMs shows a dune system spanning throughout most of the area (Fig. 3a), offering better natural protection at Praia da Bonança and Praia de Fao, given the higher topographic heights there, up to 18.23 m. The northern stretch shows less natural resilience, with most of the beachfront areas located below 10 m height. The combined effect of SLR and waves is projected to change the DTMs, mainly by moving the profiles landward, while reducing the natural strength of the dune system (Fig. 4a). In fact, by 2070 (2100), the topographic heights are projected to top at 14.9 m (15.6 m) and 14.9 m (14.6 m), under RCP4.5 and RCP8.5, respectively. SLR is also projected to change the profiles facing the Cávado River estuary, further weakening the northernmost portion of the domain.

At Costa Nova (Fig. 3f–j), the reference DTM shows a long and intact

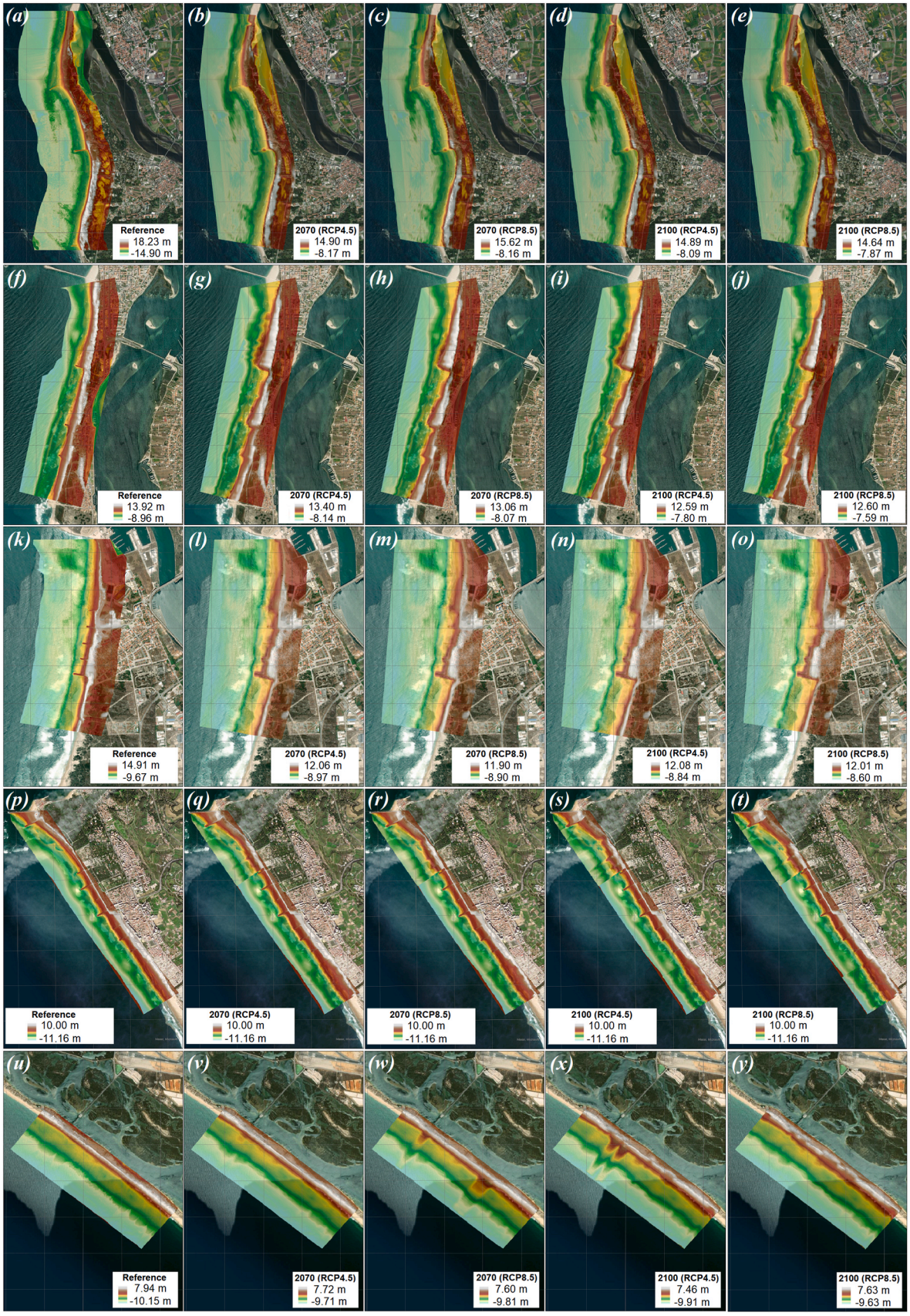

Fig. 3. (a,f,k,p,u) Reference and future projected DTMs across (a–e) Ofir, (f–j) Costa Nova, (k–o) Cova Gala, (p–t) Costa da Caparica and (u–y) Praia de Faro, by (b,g,l, q,v) 2070 under RCP4.5, (c,h,m,r,w) 2070 under RCP8.5, (d,i,n,s,x) 2100 under RCP4.5 and (e,j,o,t,y) 2100 under RCP8.5.

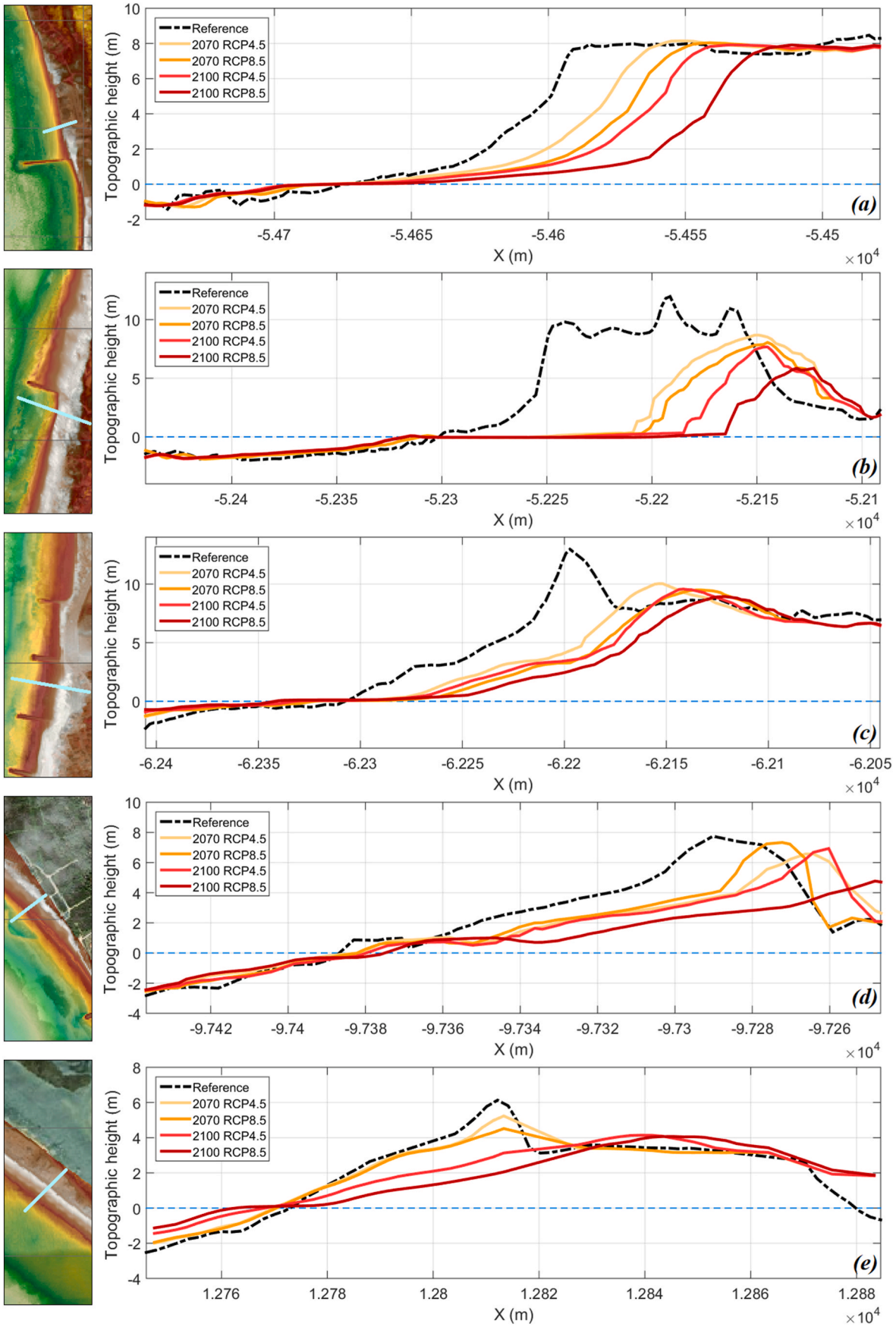

Fig. 4. Cross-section profiles for the reference and future projected DTMs across vulnerable sandy sections of the (a) Ofir, (b) Costa Nova, (c) Cova Gala, (d) Costa da Caparica and (e) Praia de Faro domains. The geographic location of the profiles is highlighted in light blue, over the reference DTMs.

dune system spanning throughout the entire domain, although wider in the northern half. The urban areas of Costa Nova are shown to be protected by natural terrain elevations of up to 13.9 m. By 2070, both DTMs (RCP4.5 and RCP8.5) display the shoreline retreat found in Part I, especially south of the groins. Although no shoreline recovery is expected north of the groins, increases in the dune thickness are projected to occur. However, not only is the future (2070) maximum topographic height lower than the reference one (13.4 m and 13.1 m for both scenarios, respectively), but the overall dune system is projected to become sectioned, with the areas south of the groins showing almost no natural protection. By 2100, while the overall behavior is projected to be similar, the fragility of (also sectioned) dune system is exacerbated (Fig. 4b). The maximum topographic heights are expected to be reduced to 12.6 m for both scenarios.

Along the Cova Gala domain, the projected DTMs (Fig. 3l–o) show similar behavioral characteristics when compared to the reference one (Fig. 3k), as in Ofir and Costa Nova. The combined effects of SLR and wave action are projected to reduce the strength of the dune systems in the northernmost and southernmost portions of the domain, by displacing them landwards while reducing their maximum topographic heights (by about 3 m; Fig. 4c). Especially for the northern dune cord, such an expected displacement might not be physically achievable, due to the proximity to the Figueira da Foz harbor infrastructure, locally increasing the vulnerability to future extreme events across all projected periods and scenarios.

At Costa da Caparica, the reference and projected DTMs are shown in Fig. 3p–t. The existence of a seawall (of about 3 km, between Praia de São João da Caparica and Praia da Saúde) along the urban front required a slightly different approach to obtain the modified DTMs, given the rigidness of that portion of the domain, unsusceptible to natural changes in the future. Therefore, the future profiles between Praia de São João da Caparica and Praia da Saúde were considered the same as the reference ones, being the modifications applied only outside this range. In the northernmost part of the domain, between Praia da Cova do Vapor and Praia de São João da Caparica, the retreat identified in Part I is also represented here, by a complete disruption of the dune cord, increasing the exposure of inland areas to extreme events (Fig. 4d). There, the maximum topographic height is projected to reduce from approximately 10 m (reference; Fig. 3p) to less than 6 m by 2100 under RCP8.5 (Fig. 3t). A reduction in the natural resilience of the southernmost dune system is also projected to occur, although less intense than in the northern areas of the domain.

Finally, at Praia de Faro, the reference DTM shows a long and wide dune system, between the Atlantic Ocean and the Ria Formosa (Fig. 3u). In the context of rising sea levels and constant wave action, while slight shoreline retreat is expected, in accordance with the results of Part I, no major changes in the projected DTMs are identified, besides a slight but consistent reduction in its maximum vertical elevation, and a landward rollover process (Fig. 4e).

3.2. Future projected extreme coastal flooding

At each key-location, the TWL components were determined considering: 1) the SLR 21-member ensemble projected CDFs, extracted at the closest grid-point to each key-location; 2) tide model projections for Viana do Castelo harbor (Ofir), Aveiro harbor (Costa Nova), Figueira da Foz harbor (Cova Gala), Cascais harbor (Costa da Caparica) and Faro harbor (Praia de Faro); and 3) the SSL CDFs corresponding to the 6-member ensemble of SSL projections, at the closest grid-point to each key-location. Upon evaluation of the overall detrended tidal projections through comparison with historical records, the local projected TWL 25-year RP values were extracted from the combined CDFs for each of the future periods and scenarios.

3.2.1. Ofir

For the Ofir key-location, Fig. SM39 in the SM shows the combined TWL components' CDFs for each future projected period and scenario, being the final values summarized in Table 1. Overall, the projections indicate an increase in the TWL values towards the end of the 21st century for both scenarios, although larger for the RCP8.5 than for the RCP4.5. The ensemble 99th percentile range for projected wave energy conditions shows, for both scenarios, an increase in the magnitude of the associated H_S values, ranging from 3.69 m to 5.88 m for 2071–2100 under the RCP8.5 scenario, compatible with ever-higher extreme H_S values in the expected future. While the T_p associated to the 99% percentile energy is projected to slightly decrease, the associated *MWD* range is expected to become narrower towards the end of the 21st century, between 270°–283° (RCP4.5) and 281°–286° (RCP8.5). Such behavior is compatible with a projected decrease in the frequency of occurrence of north-westerly storm events (Lemos et al., 2021a).

Fig. 5 shows the future projected extreme coastal flooding extension at Ofir, for the 2041–2070 and 2071–2100 future periods, under the RCP4.5 and RCP8.5 scenarios. Here, the coastal profile assumes different orientations, generally ranging from 250° to 280°. Therefore, the relevance of the incoming *MWD* on the coastal flooding results for each coastal section is enhanced, in comparison with the H_S and T_p values. For that reason, in Fig. 5a, the extension of flooding from the minimum TWL and wave energy conditions (incoming from 256°) exceeds the remaining mean and maximum ones (incoming from 276° and 294°, respectively). By 2070, under RCP4.5, the maximum flooding extent profiles are able to overtop the dune system at Ofir and produce flooding inland, along urbanized area, especially at Praia de Ofir and Praia da Bonança. For the RCP8.5 scenario, by 2070 (Fig. 5b), the three maximum flooding extents assume similar positioning, with the *MWD* associated to each group promoting a balancing of the resulting floodings. Nevertheless, urbanized areas near Praia de Ofir and Praia da Bonança are consistently projected to be directly affected, up to 120 m inland from the reference (2018) shorelines (LP1).

By the end of the 21st century, under the RCP4.5 scenario (Fig. 5c), flooding is consistently expected to reach locations further inland, in comparison with the results for 2070. The most affected portion of the area corresponds to the northern half of Praia de Ofir, south of the first groin, where flooding is not only projected to reach habitational area facing the sea, but also areas facing the Cávado River estuary, approximately 200 m from the reference shorelines, under the WAVES2 and

Table 1
Representative TWLs (relative to the National Vertical Datum CASCAIS1938; m) and wave parameters (H_S, T_p and *MWD*) used to force the XBeach at the Ofir key-location.

	Ofir		
	2041–2070 (RCP4.5)		
TWL (m)		2.95	
	WAVES1	WAVES2	WAVES3
H_S (m)	5.10	5.22	5.35
T_p (s)	13.2	14.9	17.8
MWD (°)	257	276	294
	2041–2070 (RCP8.5)		
TWL (m)		2.95	
	WAVES1	WAVES2	WAVES3
H_S (m)	4.76	5.16	5.57
T_p (s)	13.1	14.7	15.2
MWD (°)	277	283	291
	2071–2100 (RCP4.5)		
TWL (m)		3.12	
	WAVES1	WAVES2	WAVES3
H_S (m)	4.88	5.21	5.73
T_p (s)	13.2	14.2	14.9
MWD (°)	283	270	280
	2071–2100 (RCP8.5)		
TWL (m)		3.25	
	WAVES1	WAVES2	WAVES3
H_S (m)	3.69	5.05	5.88
T_p (s)	15.4	14.9	15.0
MWD (°)	286	281	283

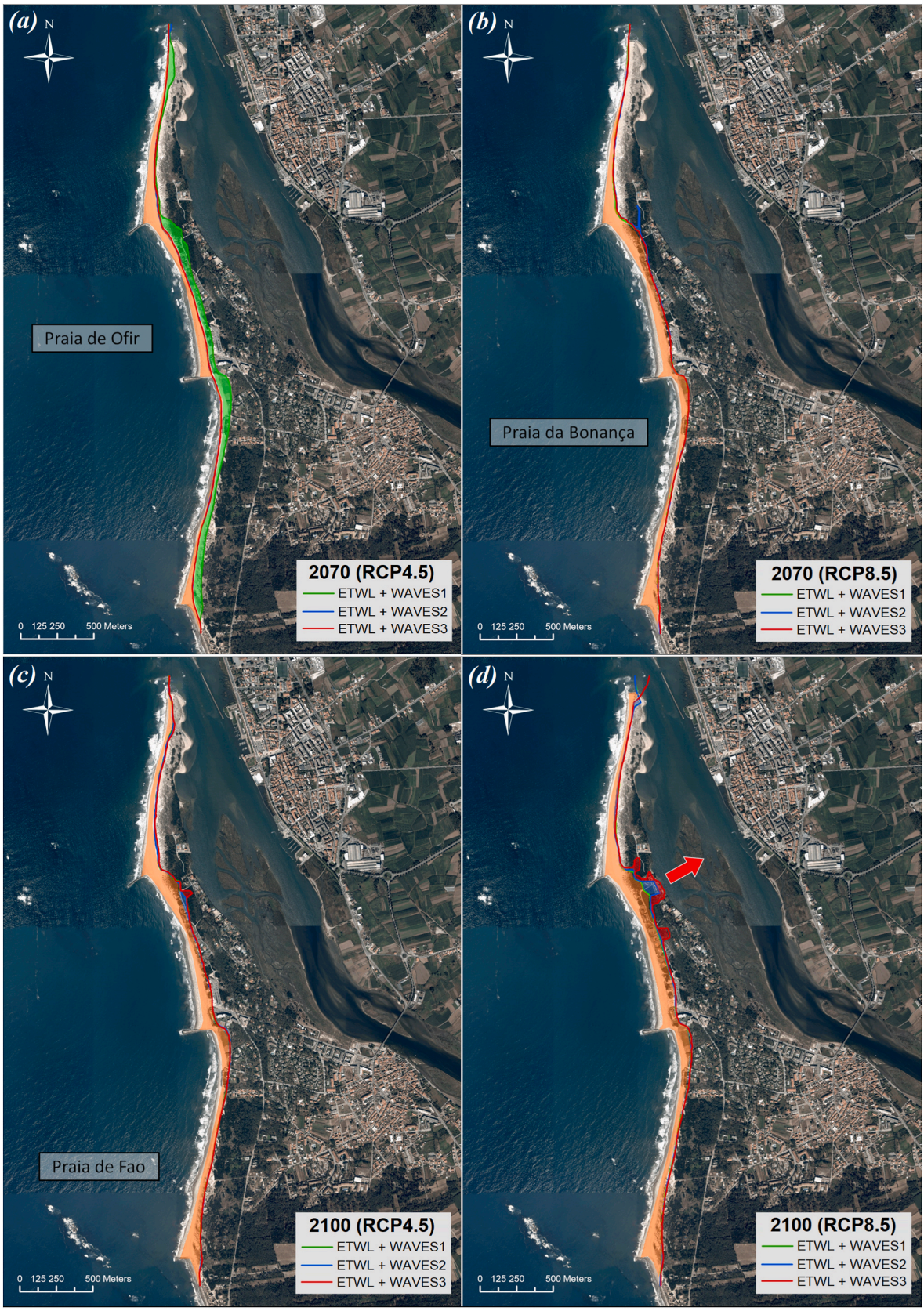

Fig. 5. Future projected extreme coastal flooding at Ofir, considering a 25-year RP TWL value (ETWL) and three levels of 99th percentile nearshore wave energy conditions (WAVES1, WAVES2 and WAVES3 – ensemble uncertainty), over the projected DTMs by (a) 2070 RCP4.5, (b) 2070 RCP8.5, (c) 2100 RCP4.5 and (d) 2100 RCP8.5. Shading represents the flooded area departing from the reference (2018) shoreline. Green, blue and red shadings refer to areas projected to be flooded under the WAVES1, WAVES2 and WAVES3 ensemble projections, respectively. Orange shading refers to areas projected to be consistently flooded under two or three extreme wave energy conditions simultaneously.

WAVES3 ensemble conditions. Finally, under RCP8.5, widespread coastal flooding is projected under extreme conditions in Fig. 5d, threatening all urbanized areas close to Praia de Ofir and Praia da Bonança. In fact, consistent flooding of urbanized areas facing the ocean (containing low and high-density habitational areas and commercial areas, such as stores, restaurants, and a beach resort) is projected for all TWL and extreme wave characteristics. Particularly at Praia de Ofir, WAVES3 run-up lines reach the Cávado River estuary, approximately 250 m inland from the reference shorelines. Under such a setting, a water corridor would be created between the ocean and the estuary (as depicted by the red arrow in Fig. 5d), isolating the northern portion of the Praia de Ofir into a temporary island, potentially disrupting habitability conditions.

Table 2 reveals the projected threatened area under future extreme coastal flooding conditions at Ofir, from the 2018 reference shorelines. Unsurprisingly, lost area is greater by the end of the 21st century under the RCP8.5, reaching 0.270 km^2 under the high-end WAVES3 energy conditions. Nevertheless, for the RCP4.5 WAVES1 setting, with southwesterly incoming waves, the projected lost area ascends to 0.214 km^2, contrasting with 0.101 km^2 and 0.103 km^2 under WAVES2 and WAVES3.

3.2.2. Costa Nova

For Costa Nova, Fig. SM40 shows the combined TWL components' CDFs for each future projected period and scenario, being the final values summarized in Table 3, along with the remaining forcing conditions. Projections indicate an increase in the TWL values towards the end of the 21st century for both scenarios and a slight decrease in the 99th percentile H_S for the RCP4.5 scenario. Nevertheless, for this scenario, the extreme T_p values are projected to increase, up to 17.70 s. It is worth noticing that the higher-threshold wave energy conditions (WAVES3) show, for all instances, a greater southerly component than their lower-threshold (WAVES1) counterparts, in accordance with the projected decrease in northwesterly extreme wave events (LP1).

The future projected extreme coastal flooding extensions at Costa Nova are shown in Fig. 6. Under RCP4.5 by 2070 (Fig. 6a), the most vulnerable locations along the domain are those immediately South of the groins, where erosion was shown to be more severe (LP1). In most of the locations, the extreme TWL and wave conditions by 2070 under the RCP4.5 scenario are not able to overtop the dune system at Praia de Costa Nova – Norte and Praia da Barra. However, at Praia de Costa Nova – Sul, South of the third groin, overtopping and flooding of urban area is projected to occur considering the higher-threshold WAVES3 energy conditions, affecting populated areas until Avenida da Bela Vista. Such projection is, nevertheless, associated with a low probability of occurrence. For the RCP8.5, by 2070 (Fig. 6b), while the extreme run-up lines are generally positioned further inland than their RCP4.5 counterparts, due to higher SLR values, here no flooding of urban area is projected to occur. Such difference is related to lower extreme wave energies projected for the ensemble members under RCP8.5. In fact, while the maximum H_S is projected to increase, from 7.34 m to 7.49 m, T_p is projected to decrease from 16.07 s to 14.90 s.

By 2100, under the RCP4.5 scenario (Fig. 6c), flooding is projected further inland, overtopping the dune system at several locations, namely at Praia de Costa Nova – Norte, south of the first groin, but also south of Praia da Barra and at Praia de Costa Nova – Sul. Especially in this last location, flooding is expected for both the WAVES2 and WAVES3 ensemble conditions, corresponding to flooding of up to 0.018 km^2 of urban area, towards Avenida José Estevão, facing the opposite shore of Costa Nova and the inland waters of Ria de Aveiro. Considering the RCP8.5 scenario, Fig. 6d shows serious a threat for Costa Nova's population, infrastructures and natural habitats by the end of the 21st century. Across the entire domain, several bulbs of extreme flooding inside urbanized areas are expected. Near Praia de Costa Nova – Norte, the ensemble run-up lines range from 150 m (WAVES1) to 350 m (WAVES3) inland, corresponding to flooding from Avenida Fernandes Lavrador up to Parque de Campismo da Barra. Further South, flooding is projected to reach populated areas West of Avenida José Estêvão, under the three extreme energy levels. At Praia de Costa Nova – Sul, urban flooding is also projected to occur under both WAVES2 and WAVES3, adding up to 0.004 km^2 and 0.028 m^2, respectively.

Considering the entire Costa Nova domain, Table 4 shows that projected coastal flooding extent under extreme TWL and wave conditions is projected to increase towards 2100, especially under RCP8.5, up to 0.385 km^2. Note that although the shoreline is mostly projected to be facing the 280°-300° range (WNW; LP1), erosion is expected to be greater south of the groins. The resulting shoreline discontinuities (also visible in Fig. 6) may lead to an increase in the exposure of the adjacent areas to westerly and southwesterly extreme wave events. Thus, under WAVES3 conditions, by 2100 (RCP8.5), results are substantially worse than by 2070 for the same event category and scenario, despite the relatively small difference in the projected TWLs (3.02 m versus 2.72 m). Such difference is mostly related to the associated *MWD* s, fixed at 265.16° (2100) and 284.08° (2070).

3.2.3. Cova Gala

At Cova Gala, Fig. SM41 in the SM shows the combined TWL components' CDFs for each future projected period and scenario. The final values are summarized in Table 5, along with the remaining forcing conditions. Until the end of the 21st century, the TWL is projected to increase, mainly due to SLR, yet the extreme wave energy conditions are

Table 2
Projected threatened area by extreme coastal flooding at Ofir, from the reference (2018; LP1) shorelines, for each future period and scenario. "ETWL" stands for "extreme TWL", corresponding to the 25-year RP levels, and "WAVES1" to "WAVES3" refer to the three ensemble *E* 99th percentile levels (lower-threshold, ensemble mean and higher-threshold).

Flooded area from reference (2018) shoreline – Ofir (km^2)				
	2041–2070 (RCP4.5)	2041–2070 (RCP8.5)	2071-2100 (RCP4.5)	2071-2100 (RCP8.5)
ETWL + WAVES1	0.214	0.158	0.190	0.233
ETWL + WAVES2	0.101	0.159	0.193	0.240
ETWL + WAVES3	0.103	0.158	0.194	0.253

Table 3
Same as in Table 1, but for Costa Nova.

Costa Nova			
2041–2070 (RCP4.5)			
TWL (m)		2.72	
	WAVES1	WAVES2	WAVES3
H_S (m)	5.75	6.31	7.34
T_p (s)	13.1	13.5	16.1
MWD (°)	291	285	275
2041–2070 (RCP8.5)			
TWL (m)		2.72	
	WAVES1	WAVES2	WAVES3
H_S (m)	6.07	6.06	7.49
T_p (s)	11.9	14.4	14.9
MWD (°)	294	285	284
2071–2100 (RCP4.5)			
TWL (m)		2.87	
	WAVES1	WAVES2	WAVES3
H_S (m)	5.46	6.10	6.89
T_p (s)	13.5	13.9	17.7
MWD (°)	292	286	287
2071–2100 (RCP8.5)			
TWL (m)		3.02	
	WAVES1	WAVES2	WAVES3
H_S (m)	6.09	6.30	7.39
T_p (s)	11.1	13.1	14.8
MWD (°)	277	281	265

Fig. 6. Similar to Fig. 5, but for the Costa Nova key-location.

Table 4
Same as in Table 2, but for Costa Nova.

Flooded area from reference (2018) shoreline – Costa Nova (km^2)				
	2041–2070 (RCP4.5)	2041–2070 (RCP8.5)	2071-2100 (RCP4.5)	2071-2100 (RCP8.5)
ETWL + WAVES1	0.138	0.161	0.196	0.291
ETWL + WAVES2	0.137	0.162	0.200	0.344
ETWL + WAVES3	0.147	0.169	0.227	0.401

Table 5
Same as in Table 1, but for Cova Gala.

Cova Gala			
2041–2070 (RCP4.5)			
TWL (m)		2.84	
	WAVES1	WAVES2	WAVES3
H_S (m)	4.67	5.10	4.96
T_p (s)	12.2	12.5	14.3
MWD (°)	297	287	282
2041–2070 (RCP8.5)			
TWL (m)		2.89	
	WAVES1	WAVES2	WAVES3
H_S (m)	4.67	4.94	5.24
T_p (s)	13.5	13.3	12.7
MWD (°)	298	289	290
2071–2100 (RCP4.5)			
TWL (m)		2.99	
	WAVES1	WAVES2	WAVES3
H_S (m)	4.07	4.92	5.17
T_p (s)	15.0	13.0	13.1
MWD (°)	282	288	291
2071–2100 (RCP8.5)			
TWL (m)		3.17	
	WAVES1	WAVES2	WAVES3
H_S (m)	4.44	4.86	5.08
T_p (s)	14.5	13.3	13.6
MWD (°)	291	295	297

projected to become slightly weaker, except for the ensemble higher-energy-threshold (WAVES3) under the RCP4.5.

Fig. 7 depicts the future projected extreme coastal flooding conditions at the Cova Gala key-location. Like in the previous areas, the most vulnerable locations along the domain are generally located South of the groins. It is worth mentioning that a groin is also located immediately North of the domain (although not visible), affecting its northernmost part. By 2070, under RCP4.5 (Fig. 7a), results show no major coastal flooding occurrences in urbanized area, although the groins and most of the beach areas are consistently projected to become temporarily submerged under extreme TWL and wave conditions. Communication routes closer to the beach may also suffer from flooding under extreme conditions, especially in Praia do Cabedelo and Praia do Hospital. For the RCP8.5 (Fig. 7b), differences by 2070 are marginal, although showing a consistent inland displacement of the maximum run-up lines. Despite the higher TWLs, extreme wave conditions are not able to overtop the main artificial and natural defense structures at Cova Gala.

By 2100, flooding is projected further inland for both scenarios, overtopping the dune system at several locations, namely at Praia do Cabedelo, Praia do Hospital, and partially at Praia de Cova Gala – Norte and Praia de Cova Gala – Sul. Although no urban area is projected to become directly affected by extreme flooding events by the end of the 21st century under RCP4.5 (Fig. 7c), maximum run-up lines are projected to just a few meters away from habitational areas and roads. Finally, for the RCP8.5 scenario, extreme coastal flooding projections point to strong physical impacts on structures near Praia do Hospital and Praia de Cova Gala – Norte, and partially at Praia de Cova Gala – Sul. Especially near Praia de Hospital, the parking lot which provides both access to the beach and to the hospital is projected to become temporarily flooded under extreme TWL and wave energy conditions. Maximum run-up lines are projected to lay closer to urban areas than in the previous scenarios, partially flooding habitational buildings at the northern end of Praia de Cova Gala – Sul. It should be noted that, within the current assessment, the 99th percentile energy conditions are, by definition, exceeded 14 times each year, which may locally produce extreme coastal flooding deeper inside urbanized areas.

The projected area to be threatened under extreme coastal flooding at Cova Gala is described in Table 6. Overall, extents tend to be smaller here than at Ofir and Costa Nova, mainly due to the natural configuration of the shoreline and artificial protection measures (seawalls) implemented near most urbanized areas. By 2070 (2100), flood extents range from 0.086 km^2 to 0.108 km^2 (0.111 km^2–0.158 km^2).

3.2.4. Costa da Caparica

Along Costa da Caparica, Fig. SM42 shows the combined TWL components' CDFs for both projected periods and scenarios, being the final values summarized in Table 7. Overall, similarly to the previous key-locations, the projections indicate an increase in the TWL values towards the end of the 21st century for both scenarios, mainly related to the SLR. The ensemble 99th percentile range for projected wave energy conditions shows, for both scenarios, a slight increase in the maximum associated H_S values, but a decrease in the minimum ones, compatible with a greater range of uncertainty towards the end of the 21st century regarding the extreme events. The T_p associated to the 99% percentile energy is projected to remain relatively unchanged, especially after 2070. Regarding the *MWD*, a slight northward (counterclockwise) rotation trend is visible towards the end of the 21st century in both scenarios. Such behavior was already inferred from the projected longshore sediment transport projections along the area (LP1).

The future projected extreme coastal flooding extensions are shown in Fig. 8, similar to Fig. 5, but for Costa da Caparica. Overall, the behavior differs considerably between the areas protected by the seawall, and the remaining ones. By 2070, while the seawall, within its current configuration, is able to withstand the water levels generated by the considered extreme conditions, for all ensemble scenarios except for WAVES3 under RCP8.5, the sandy beaches outside its range are projected to become threatened along their entire extension. At Praia de São João da Caparica, for example, extreme coastal flooding is projected to overtop the dune system, compromising several food service areas (restaurants, bars and lounges) and parking lots (under both scenarios; Fig. 8a and b). Nevertheless, about 1 km South, at Praia do Inatel, projections indicate slightly prograded extreme run-up lines, compatible with the projected shoreline accretion in the area (LP1). Along the urbanized ocean front of Costa da Caparica, overtopping of the seawall is visible under RCP8.5 (Fig. 8b) at Praia do CDS, with flooding affecting local services (restaurants, bars), parking lots and the first row of communication routes.

By the end of the 21st century, flooding is consistently expected to extend further inland. At Praia de São João da Caparica, extreme coastal flooding is projected up to 250 m onshore from the reference (2018) shoreline, additionally threatening communication routes well beyond the dune system. While under RCP4.5 forcing conditions, no overtopping of Caparica's seawall is projected, between Praia do Tarquínio-Paraíso and Nova Praia, maximum run-up lines are projected to move towards the base of the seawall.

By 2100, under RCP8.5, widespread extreme coastal flooding is projected at Costa da Caparica, especially considering WAVES3 conditions. At Praia de São João da Caparica, flooding is projected the threaten all current infrastructure in the area. Further South, at Praia do Inatel, maximum run-up lines are expected to reach the base of the seawall, except under WAVES1 conditions. Even within these expected conditions, Praia do Inatel shows, considering the current coastal configuration, enhanced resiliency to the impacts of climate change. While the northernmost portion of the seawall is projected to withstand

Fig. 7. Similar to Fig. 5, but for the Cova Gala key-location.

Table 6
Same as in Table 2, but for Cova Gala.

Flooded area from reference (2018) shoreline – Cova Gala (km^2)				
	2041–2070 (RCP4.5)	2041–2070 (RCP8.5)	2071-2100 (RCP4.5)	2071-2100 (RCP8.5)
ETWL + WAVES1	0.086	0.108	0.111	0.158
ETWL + WAVES2	0.087	0.096	0.130	0.156
ETWL + WAVES3	0.088	0.098	0.111	0.142

Table 7
Same as in Table 1, but for Costa da Caparica.

Costa da Caparica			
2041–2070 (RCP4.5)			
TWL (m)		2.77	
	WAVES1	WAVES2	WAVES3
H_S (m)	3.65	3.56	3.34
T_p (s)	11.0	13.5	16.7
MWD (°)	214	221	224
2041–2070 (RCP8.5)			
TWL (m)		2.81	
	WAVES1	WAVES2	WAVES3
H_S (m)	3.19	3.50	3.62
T_p (s)	13.4	13.1	13.4
MWD (°)	230	224	224
2071–2100 (RCP4.5)			
TWL (m)		2.94	
	WAVES1	WAVES2	WAVES3
H_S (m)	3.17	3.51	3.85
T_p (s)	13.8	13.4	12.3
MWD (°)	227	224	219
2071–2100 (RCP8.5)			
TWL (m)		3.08	
	WAVES1	WAVES2	WAVES3
H_S (m)	3.06	3.46	3.70
T_p (s)	12.9	13.1	13.4
MWD (°)	229	224	229

the considered future extreme conditions, along the urbanized ocean front of Costa da Caparica, run-up lines are expected further inland (especially for WAVES2 and WAVES3), directly affecting local services and urbanized areas containing high-density habitational infrastructure, up to 250 m inland. Note that, similarly to Costa Nova (Fig. 6d), flooding in densely urbanized areas may exceed the extension given by the XBeach model, since infrastructures are not considered in the projected DTMs, which may redirect the water flow further inland.

For the entire Costa da Caparica domain, Table 8 shows that projected coastal flooding extent under extreme TWL and wave conditions is projected to increase towards 2100, especially under RCP8.5, up to 0.493 km^2. Given the reduced *MWD* range at Costa da Caparica, due to its geographical location, protected by the Lisbon peninsula from stronger northwesterly swells, future projected extreme coastal flooding assumes a more homogeneous extension for all periods and scenarios compared to the Ofir, Costa Nova and Cova Gala key-locations. Nevertheless, it is generally observable that extreme conditions marked by a pure southwesterly *MWD* (approximately 225°) produce greater flooding extensions in the northermost portion of the domain, while more southerly events (within 210°-220°) affect especially the southernmost areas.

3.2.5. *Praia de Faro*

At Praia de Faro, Fig. SM43 in the SM shows the CDFs of the combined TWL components for each future projected period and scenario. The final values are summarized in Table 9, along with the remaining forcing conditions. There, while TWL values are projected to increase, which mainly related to the SLR component, extreme wave energy shows a slight projected reduction between 2070 and 2100, for both scenarios, although larger for the RCP8.5 (Table 9). This change is motivated by the H_S behavior, which is also projected to slightly decrease towards 2100, except under WAVES3 for RCP4.5. Nevertheless, these extreme conditions are projected to be accompanied by a relatively low T_p (8.86 s), culminating in lower total energy when compared to the 2070 WAVES3. Considering the incoming *MWD*, the results show relatively similar projections among the future periods and scenarios, except for the absence of southerly extreme events outside 2041–2070 under RCP4.5.

Fig. 9 shows the future projected extreme coastal flooding extension at Praia de Faro, by the end of the 2041–2070 and 2071–2100 future periods, under the RCP4.5 and RCP8.5 scenarios. At this key location, the coastal profile is consistently oriented to the southwest (approximately 225°). Nevertheless, all the projected extreme conditions are characterized by *MWD* s ranging from 155° to 178°, and therefore, none of the events hit the coast perpendicularly. Therefore, for the extreme conditions considered, the impact of H_S and T_p (and overall TWL) dominates over *MWD*. By 2070, under RCP4.5, the maximum projected flooding extensions surpass the sandy beaches, reaching the beginning of the urbanized area. Under RCP8.5, nevertheless, the first row of infrastructure is already projected to be threatened. In both instances, ensemble uncertainty related to wave energy is generally well contained.

By 2100, both scenarios depict extreme flooding to extend well over the urbanized areas. While flooding under RCP4.5 is mainly restricted to the lowest areas of Praia de Faro (essentially impacting parking lots besides the first row of infrastructure), for the RCP8.5, extreme flooding is expected to extend along and over most of the urbanized areas. Especially for the WAVES3 ensemble conditions, run-up lines reach the opposite shores of Praia de Faro, facing the Ria Formosa, approximately 140 m inland from the reference shorelines. Similarly to Ofir, under such a projection, water corridors would be created between the ocean and the Ria Formosa (as shown by the red arrows in Fig. 9d), creating a set of small, temporary islands, potentially leading to a complete disruption of normal habitability conditions.

Table 10 shows, across the entire Praia de Faro key-location, the projected coastal flooding extents under extreme TWL and wave conditions. These are projected to increase towards the end of the 21st century, for both scenarios, as revealed by the results of Fig. 9, up to 0.167 km^2 (by 2100 under RCP8.5). Results show greater extents for the RCP8.5, for which the areas projected by 2070 slightly exceed the ones for RCP4.5 by 2100.

4. Discussion and conclusions

In this work, the first consistent, ensemble-based assessment of future extreme coastal flooding along five of the Portuguese most vulnerable coastal stretches was conducted, based on a large set of CMIP5 data. A 21-member ensemble of SLR projections was used, together with a (consistent) 6-member ensemble of nearshore, bias corrected wave climate and storm surge projections, as well as local tide projections. Shoreline evolution projections from the companion Part I paper (Lemos et al., 2024a; LP1) allowed the modification of the reference DTMs, over which future extreme coastal flooding was projected. The range of physical impacts related to such extreme conditions were probabilistically quantified at five key-locations along the Portuguese coastline, based on an ensemble approach, considering high wave energy thresholds combined with moderate TWL RP values. This methodology, aligned with other studies conducted in different high-risk coastal areas globally (*e.g.*, Toimil et al., 2017; Lopes et al., 2017; Garner et al., 2017; Antunes et al., 2019; Alvarez-Cuesta et al., 2021; Ribeiro et al., 2021; Barros et al., 2022), allowed for a more precise assessment of impacts and vulnerabilities, in areas already considered sensitive to extreme events in the present day.

Fig. 8. Similar to Fig. 5, but for the Costa da Caparica key-location.

Table 8
Same as in Table 2, but for Costa da Caparica.

Flooded area from reference (2018) shoreline – Costa da Caparica (km^2)				
	2041–2070 (RCP4.5)	2041–2070 (RCP8.5)	2071-2100 (RCP4.5)	2071-2100 (RCP8.5)
ETWL + WAVES1	0.165	0.192	0.208	0.414
ETWL + WAVES2	0.168	0.193	0.210	0.440
ETWL + WAVES3	0.174	0.201	0.229	0.493

Table 9
Same as in Table 1, but for Praia de Faro.

Praia de Faro			
2041–2070 (RCP4.5)			
TWL (m)		2.72	
	WAVES1	WAVES2	WAVES3
H_S (m)	2.32	2.29	2.53
T_p (s)	8.11	10.7	9.95
MWD (°)	179	160	155
2041–2070 (RCP8.5)			
TWL (m)		2.76	
	WAVES1	WAVES2	WAVES3
H_S (m)	1.55	2.11	2.15
T_p (s)	16.3	11.4	11.8
MWD (°)	162	158	158
2071–2100 (RCP4.5)			
TWL (m)		2.89	
	WAVES1	WAVES2	WAVES3
H_S (m)	2.05	2.07	2.68
T_p (s)	9.67	12.8	8.86
MWD (°)	165	159	159
2071–2100 (RCP8.5)			
TWL (m)		3.06	
	WAVES1	WAVES2	WAVES3
H_S (m)	1.90	1.94	1.76
T_p (s)	11.2	12.8	17.1
MWD (°)	164	159	157

Currently, there is no single model able to compute all different contributions to the TWL directly. Therefore, these must be individually considered and combined (Fox-Kemper et al., 2021; Parker et al., 2023). There has been growing interest regarding the use of probabilistic approaches to assess the impacts of SLR and TWLs on coastal areas (*e.g.*, Leijala et al., 2018; Antunes et al., 2019; Jevrejeva et al., 2019; Liu et al., 2020; Gori and Lin, 2022). These yield several advantages over deterministic ones, incorporating and better accounting for uncertainties (Toimil et al., 2021) and variability associated to climate change, oceanographic processes, model assumptions and input data (Marcy et al., 2011; Antunes et al., 2019). Here, a probabilistic method was considered to provide a numerical solution in the estimation of representative RPs of extreme TWLs, based on the probabilistic combination of the cumulative density functions of SLR, tides and storm surges. By quantifying physical impacts probabilistically, this approach was able to differentiate areas according to their vulnerability, allowing the development targeted adaptation strategies.

Regarding future morphological evolution at the key-locations, the PaCR algorithm was shown to be able to reproduce the shoreline retreat obtained in LP1 along the cross-shore profiles, while building the projected 3-dimensional topographic model of all key-locations. Overall, the projected DTMs revealed enhanced vulnerabilities arising from SLR and wave action. By 2070 (2100), the natural protection of the shoreline along all key-locations is projected to be reduced, on average, by 13.3% (12.3%) under the RCP4.5 scenario, and by 10.5% (12.5%) under RCP8.5, considering the differences between the reference and future projected DTMs' maximum topographic heights (Figs. 3 and 4).

The future projected extreme coastal flooding, as depicted by XBeach forced by 25-year TWL return values associated to three levels of 99th percentile wave energy conditions, was shown in Figs. 5–9. Given the natural and artificial heterogeneities of each key-location, the XBeach was run in 2DH mode, allowing the representation of the directional spreading of waves and their shadowing by morphological features or structures (Nahon et al., 2023). The enhanced vulnerabilities of the projected DTMs in comparison with the reference ones promoted the occurrence of coastal flooding events. In fact, it should be noted that no major coastal flooding occurrences were identified considering the future projected extreme TWL and wave conditions over the reference (historical) DTMs. A summary of the results found for each key-location in Figs. 5–9 is provided in Table 11.

At Costa Nova, extreme coastal flooding was shown to be projected within urbanized areas for all future periods and scenarios. This highly vulnerable stretch of coast has been extensively studied in recent years, with compatible conclusions from several authors (Lopes et al., 2017; Antunes et al., 2019; Ferreira et al., 2020; Rocha et al., 2020; Ribeiro et al., 2021; Barros et al., 2022). Further South, in Costa da Caparica, future projections revealed in fact two critical areas: the northern portion of the domain, by 2070, at Praia de São João da Caparica (impacting uniquely local services infrastructure), and the densely urbanized areas of Costa da Caparica's oceanfront, by 2100, overtopping the seawall (especially under RCP8.5; Fig. 9d) and threatening habitational hubs, besides services and communication routes. Our results are in agreement with recent studies focusing on this area, especially when considering short-to-moderate projected return periods (Antunes et al., 2019; Ferreira et al., 2021a; Melet et al., 2021). Finally, at Praia de Faro, local infrastructures were shown to be progressively threatened by the projected changes in water levels towards 2100, especially under the high-end RCP8.5 scenario. In case no additional measures are taken to mitigate the local impacts of the extreme events considered, permanent habitability conditions along most of the urbanized areas within Praia de Faro may become extensively disrupted (Fig. 9). These results are in accordance with Ferreira et al. (2021b), which shows a consistent projected increase in the overwash potential at Praia de Faro.

Throughout the five key-locations (approximately 14 km of coastline), the projected threatened area, expected to become flooded under extreme TWL and wave conditions, ascends to 0.657 km^2 (0.738 km^2) by 2070 under RCP4.5 (RCP8.5), and 0.841 km^2 (1.47 km^2) by 2100 under RCP4.5 (RCP8.5), as shown in Table 12. It should be noted that the 99th wave energy percentile could, by definition, be exceeded within the considered TWL conditions (which may also be occasionally surpassed). In such conditions, coastal flooding could potentially extend further inland, especially if associated to a cross-shore incoming direction of wave propagation. Moreover, although coastal protection infrastructures were considered in the DTMs (*e.g.*, seawalls), buildings over land were not represented, which may have influenced the landward expression of the projected flooding extent (Schubert and Sanders, 2012; LeRoy et al., 2015; Gallien et al., 2018).

Overall, extreme wave energy synchronized with increased TWLs (resulting essentially from SLR, but also from the joint occurrence of high spring tides or storm surge conditions) in the context of weaker natural protection structures (*e.g.*, fragilized dune systems), may lead to unprecedented coastal flooding in the future, if no additional coastal protection and adaptation measures are implemented. Episodic extreme flooding could be responsible for most of the disrupting effects in living conditions along the Portuguese coastline during the 21st century, potentially leading to the inevitable implementation of hard defense structures, or even the abandonment of the shoreline long before permanent inundation takes place (Toimil et al., 2020). On the other hand, by probabilistically characterizing the future projected extreme coastal flooding patterns, our results promote the adequate development of tailored adaptation plans, fostering the sustainable evolution of the analyzed coastal sectors, based on informed decision-making.

Adaptation measures in Portugal have been implemented since the 1960s, consisting mostly of hard defense structures, such as groins and

Fig. 9. Similar to Fig. 5, but for the Praia de Faro key-location.

Table 10
Same as in Table 2, but for Praia de Faro.

Flooded area from reference (2018) shoreline – Praia de Faro (km^2)				
	2041–2070 (RCP4.5)	2041–2070 (RCP8.5)	2071-2100 (RCP4.5)	2071-2100 (RCP8.5)
ETWL + WAVES1	0.055	0.108	0.111	0.166
ETWL + WAVES2	0.056	0.109	0.110	0.167
ETWL + WAVES3	0.057	0.112	0.112	0.179

seawalls, as well as artificial beach nourishment and sediment bypassing (essentially since the 1980s). The implementation of nature-based solutions has been gaining increased attention recently (Temmerman et al., 2013), especially for dune protection. Despite a slowly increasing interest nature-based approaches by the global community (Brière et al., 2018; Van Loon-Steensma et al., 2019), the rate of increase in the extreme sea levels may be too high to simply consider those approaches. As of today, artificial beach nourishment continues to be the measure of choice to maintain stable shoreline evolution in Portugal (Pinto et al., 2015, 2016, 2020, 2022). According to Parkinson and Ogurcak, (2018), artificial beach nourishments should continue to be a viable option during the next decades, but not as a long-term solution. Rather, it should be considered as a provisory measure, to gain time to implement more robust and long-term strategies, such as re-localization.

Protection and accommodation are currently the measures of choice to increase resilience of the Portuguese coastal areas against climate change. Although relocation has already been conducted in Portugal (*e.g.*, Esmoriz and Praia de Faro; Santos, 2020), many doubts about its effectiveness in the short and medium-term arise, due to extensive bureaucratic processes and the difficulties regarding legislation enforcement through the territorial management instruments in

Table 11
Summary of the main results found for each key-location along the Portuguese coastline.

Key-location	Key-results
Ofir	Projected increase in the extreme TWLs and wave energy levels towards 2100. Overtopping of the dune system and coastal flooding inland reaching urbanized area and extending up to 250 m inland (2100 under RCP8.5). Potential establishment of temporary water corridors between the ocean and the Cávado River estuary.
Costa Nova	Projected increase in the extreme TWLs and wave energy levels towards 2100. Locations immediately South of the groins are the most vulnerable, where projected erosion was shown to be more severe (LP1). Widespread coastal flooding along urban areas is expected, extending up to 350 m inland (2100 under RCP8.5). Local coastal flooding occurrences projected to occur as soon as by 2070 under RCP4.5.
Cova Gala	Projected increase in the extreme TWLs towards 2100. Extreme waves projected to become slightly weaker under RCP8.5. Locations immediately South of the groins are the most vulnerable, where projected erosion was shown to be more severe (LP1). While no overtopping of the seawall is projected, maximum run-up lines from extreme events may extend up to 150–200 m inland.
Costa da Caparica	Projected increase in the extreme TWLs towards 2100. Extreme wave energy trends unclear. Extensive coastal flooding is projected under RCP8.5, overtopping the seawall and directly affecting local services and urbanized areas containing high-density habitational infrastructure, up to 250 m inland.
Praia de Faro	Projected increase in the extreme TWLs towards 2100. Extreme waves projected to become slightly weaker for both scenarios. Nevertheless, extreme coastal flooding is projected along the urbanized areas, especially for RCP8.5. Potential establishment of temporary water corridors between the ocean and the Ria Formosa coastal lagoon.

Table 12
Projected accumulated threatened area by extreme coastal flooding from the reference (2018) shorelines, throughout the five key-locations, for each future period and scenario (similar to Tables 2, 4, 6, 8 and 10).

Flooded area from reference (2018) shoreline – All key-locations (km^2)				
	2041–2070 (RCP4.5)	2041–2070 (RCP8.5)	2071-2100 (RCP4.5)	2071-2100 (RCP8.5)
ETWL + WAVES1	0.657	0.727	0.816	1.26
ETWL + WAVES2	0.561	0.717	0.841	1.35
ETWL + WAVES3	0.570	0.738	0.873	1.47

Portugal (Santos et al., 2014). Recently, in the context of the RNA2100 project, a large multi-sectoral workshop was held, mobilizing more than 100 people, in which government decision-makers and key elements of public and private institutions were present. Upon consultation of all entities involved, it was concluded that the revision of legislation related to the territorial management instruments along with its enforcement to safeguard infrastructures, communities and ecosystems in coastal areas, is a priority measure requiring implementation in Portugal within the next decade. A proactive legislative framework, able to adapt to continuously changing conditions, is needed. As changes are expected to continue well beyond the end of the 21st century (Lyon et al., 2022), any measure of coastal protection must consider additional levels of protection to be implemented in the longer-term (beyond 2100). In this context, relocation was deemed ultimately necessary along the most vulnerable coastal urban areas, essentially from the last third of the 21st century onwards, from where its cost-effectiveness should become advantageous throughout most of the highly vulnerable areas.

As the need to design a complete climate change assessment for the Portuguese coastal areas increases, our results, based on multi-model, multi-process and multi-scenario approaches, allow the translation of the local dynamical results into a large-scale probabilistic approach to ultimately produce coastal vulnerability and risk cartography, considering the uncertainties associated to modelling efforts, climate change scenarios, DTMs, and particularly to the SLR, tides, SSLs and wave climate projections. Nevertheless, several limitations still need to be overcome, especially due to the multiple modelling platforms required to perform the full analysis (initiated in LP1), and to the unconsidered small- and short-scale feedbacks between hydrodynamic forcing and morphological response, usually neglected in climate projections due to the long simulation periods. Future studies should emphasise on the consistency between datasets, the continuity within the modelled processes and the use of probabilistic approaches instead of deterministic ones in the context of coastal erosion and flooding.

CRediT authorship contribution statement

Gil Lemos: Writing – original draft, Validation, Methodology, Investigation, Formal analysis, Conceptualization. **Ivana Bosnic:** Writing – review & editing, Software, Investigation, Formal analysis. **Carlos Antunes:** Writing – review & editing, Supervision, Formal analysis, Data curation. **Michalis Vousdoukas:** Writing – review & editing, Data curation. **Lorenzo Mentaschi:** Writing – review & editing, Data curation. **Miguel Espírito Santo:** Software, Methodology. **Vanessa Ferreira:** Software, Methodology. **Pedro M.M. Soares:** Writing – review & editing, Project administration, Funding acquisition.

Declaration of competing interest

The authors declare that they have no known competing financial interests or personal relationships that could have appeared to influence the work reported in this paper.

Acknowledgements

The authors would like to acknowledge the financial support of the Portuguese Fundação para a Ciência e a Tecnologia (FCT) I.P./MCTES through national funds (PIDDAC) – UIDB/50019/2020 (https://doi.org/10.54499/UIDB/50019/2020), UIDP/50019/2020 (https://doi.org/10.54499/UIDP/50019/2020), and LA/P/0068/2020 (https://doi.org/10.54499/LA/P/0068/2020). The authors also acknowledge the EEA Financial Mechanism 2014–2021 and the Portuguese Environment Agency through Pre defined Project 2 National Roadmap for Adaptation XXI (PDP 2).

Appendix A. Supplementary data

Supplementary data to this article can be found online at https://doi.org/10.1016/j.oceaneng.2024.118448.

References

Alvarez-Cuesta, M., Toimil, A., Losada, I.J., 2021. Modelling long-term shoreline evolution in highly anthropized coastal areas. Part 2: assessing the response to climate change. Coast Eng. 168, 103961 https://doi.org/10.1016/j.coastaleng.2021.103961.

Arns, A., Wahl, T., Wolff, C., Vafeidis, A.T., Haigh, I.D., Woodworth, P., Niehüser, S., Jensen, J., 2020. Non-linear interaction modulates global extreme sea levels, coastal flood exposure, and impacts. Nat. Commun. 11 (1), 1918. https://doi.org/10.1038/s41467-020-15752-5.

Antunes, C., 2007. Previsão de Marés dos Portos Principais de Portugal. FCUL Webpage. http://webpages.fc.ul.pt/~cmantunes/hidrografia/hidro_mares.html.

Antunes, C., 2014. Eventos Extremos e a variação do Nível do mar. Actas das 3.as Jornadas de Engenharia Hidrográfica 33–36. https://www.hidrografico.pt/jornada/4.

Antunes, C., 2017. Metodologia de Aplicação da Regra de Recuo da Linha de Costa à Modelação do MDT - Regra de Bruun modificada (non published monography).

Antunes, C., Lemos, G., 2024. Probabilistic Approach to Combine Sea Level Rise, Tide, and Storm Surge into Representative Return Periods of Extreme Total Water Levels. Under review at Estuarine, Coastal and Shelf Science.

Antunes, C., Rocha, C., Catita, C., 2019. Coastal flood assessment due to sea level rise and extreme storm events: a case study of the atlantic coast of Portugal's mainland. Geosciences 9 (5), 239. https://doi.org/10.3390/geosciences9050239.

Ardhuin, F., et al., 2010. Semiempirical dissipation source functions for ocean waves. Part I: definition, calibration, and validation. J. Phys. Oceanogr. 40 (9), 1917–1941. https://doi.org/10.1175/2010jpo4324.1.

Baldassarre, G.D., Schumann, G., Bates, P.D., Freer, J.E., Beven, K.J., 2010. Flood-plain mapping: a critical discussion of deterministic and probabilistic approaches. Hydrological Sciences Journal 55 (3), 364–376.

Barros, J.L., Tavares, A.O., Santos, P.P., Freire, P., 2022. Enhancing a coastal territorial vulnerability index: anticipating the impacts of coastal flooding with a local scale approach, 50 (5), 6–25. https://doi.org/10.1080/08920753.2022.2107858.

Bengtsson, L., Hodges, K.I., Keenlyside, N., 2009. Will extratropical storms intensify in a warmer climate? J. Clim. 22, 2276–2301. https://doi.org/10.1175/2008JCLI2678.1.

Bento, V.A., Russo, A., Vieira, I., Gouveia, C.M., 2023. Identification of forest vulnerability to droughts in the Iberian Peninsula. Theor. Appl. Climatol. 152, 559–579. https://doi.org/10.1007/s00704-023-04427-y.

Booij, N., Ris, R.C., Holthuijsen, L.H., 1999. A third-generation wave model for coastal regains: 1. Model description and validation. J. Geophys. Res. 104 (C4), 7649–7666. https://doi.org/10.1029/98JC02622.

Brière, C., Janssen, S.K.H., Oost, A.P., et al., 2018. Usability of the climate-resilient nature-based sand motor pilot, The Netherlands. J Coast Conserv 22, 491–502. https://doi.org/10.1007/s11852-017-0527-3.

Camelo, J., Mayo, T.L., Gutmann, E.D., 2020. Projected climate change impacts on hurricane storm surge inundation in the coastal United States. Frontiers in Built Environment 6, 207pp. https://doi.org/10.3389/fbuil.2020.588049.

Camus, P., Haigh, I.D., Nasr, A.A., Wahl, T., Darby, S.E., Nicholls, R.J., 2021. Regional analysis of multivariate compound coastal flooding potential around Europe and environs: sensitivity analysis and spatial patterns. Nat. Hazards Earth Syst. Sci. 21, 2021–2040. https://doi.org/10.5194/nhess-21-2021-2021.

Cardoso, R.M., Lima, D.C.A., Soares, P.M.M., 2023. How persistent and hazardous will extreme temperature events become in a warming Portugal? Weather Clim. Extrem. 41, 100600 https://doi.org/10.1016/j.wace.2023.100600.

Catto, J.L., Shaffrey, L.C., Hodges, K.I., 2011. Northern hemisphere extratropical cyclones in a warming climate in the HiGEM high-resolution climate model. J. Clim. 24, 5336–5352. https://doi.org/10.1175/2011JCLI4181.1.

Chen, W.-B., Chen, H., Hsiao, S.-C., Chang, C.-H., Lin, L.-Y., 2019. Wind forcing effect on hindcasting of typhoon-driven extreme waves. Ocean Eng. 188, 106260 https://doi.org/10.1016/j.oceaneng.2019.106260.

ECMWF, 2016. IFS documentation CY41R2. https://www.ecmwf.int/node/16651.

Ferreira, J.C., Cardona, F.S., Santos, C.J., Tenedório, J.A., 2021b. Hazards, Vulnerability, and Risk Analysis on Wave Overtopping and Coastal Flooding in Low-Lying Coastal Areas: The Case of Costa da Caparica, Portugal. Water 13 (2), 237.

Ferreira, A.M., Coelho, C., Narra, P., 2020. Coastal erosion risk assessment to discuss mitigation strategies: Barra-Vagueira, Portugal. Nat. Hazards. https://doi.org/10.1007/s11069-020-04349-2.

Ferreira, Ó., Kupfer, S., Costas, S., 2021a. Implications of sea-level rise for overwash enhancement at South Portugal. Nat. Hazards 109, 2221–2239.

Feyen, L., Ciscar Martinez, J., Gosling, S., Ibarreta Ruiz, D., Soria Ramirez, A., Dosio, A., Naumann, G., Russo, S., Formetta, G., Forzieri, G., Girardello, M., Spinoni, J., Mentaschi, L., Bisselink, B., Bernhard, J., Gelati, E., Adamovic, M., Guenther, S., De Roo, A., Cammalleri, C., Dottori, F., Bianchi, A., Alfieri, L., Vousdoukas, M., Mongelli, I., Hinkel, J., Ward, P., Gomes Da Costa, H., De Rigo, D., Liberta, G., Durrant, T., San-Miguel-Ayanz, J., Barredo Cano, J., Mauri, A., Caudullo, G., Ceccherini, G., Beck, P., Cescatti, A., Hristov, J., Toreti, A., Perez Dominguez, I., Dentener, F., Fellmann, T., Elleby, C., Ceglar, A., Fumagalli, D., Niemeyer, S., Cerrani, I., Panarello, L., Bratu, M., Després, J., Szewczyk, W., Matei, N., Mulholland, E., Olariaga-Guardiola, M., 2020. Climate Change Impacts and Adaptation in Europe, EUR 30180 EN. Publications Office of the European Union, Luxembourg. https://doi.org/10.2760/171121,JRC119178, 978-92-76-18123-1.

Fox-Kemper, B., Hewitt, H.T., Xiao, C., Aðalgeirsdóttir, G., Drijfhout, S.S.D., Edwards, T. L., Golledge, N.R., Hemer, M., Kopp, R.E., Krinner, G., Mix, A., Notz, D., Nowicki, S., Nurhati, I.S., Ruiz, L., Sallée, J.-B., Slangen, A.B.A., Yu, Y., 2021. Ocean, cryosphere and sea level change. In: Masson-Delmotte, V., Zhai, P., Pirani, A., Connors, S.L., Péan, C., Berger, S., Caud, N., Chen, Y., Goldfarb, L., Gomis, M.I., Huang, M., Leitzell, K., Lonnoy, E., Matthews, J.B.R.T., Maycock, K., Waterfield, T., Yelekçi, O., Yu, R., Zhou, B. (Eds.), Climate Change 2021: the Physical Science Basis. Contribution of Working Group I to the Sixth Assessment Report of the Intergovernmental Panel on Climate Change. Cambridge University Press, Cambridge, United Kingdom and New York, NY, USA.

Garner, A.J., et al., 2017. Impact of climate change on New York City's coastal flood hazard: increasing flood heights from the preindustrial to 2300 CE. Proc. Natl. Acad. Sci. USA 114, 11861–11866.

Gallien, T., Kalligeris, N., Delisle, M.-P., Tang, B.-X., Lucey, J.T.D., Winters, M.A., 2018. Coastal flood modeling challenges in defended urban backshores. Geosciences 8 (12), 450. https://doi.org/10.3390/geosciences8120450.

Gori, A., Lin, N., 2022. Projecting Compound Flood Hazard Under Climate Change With Physical Models and Joint Probability Methods. Earth's Future 10 (12), e2022EF003097.

Haigh, I.D., Eliot, M., Pattiaratchi, C., 2011. Global influences of the 18.61 year nodal cycle and 8.85 year cycle of lunar perigee on high tidal levels. J. Geophys. Res.: Oceans 116, C6. https://doi.org/10.1029/2010JC006645.

Hay, L.E., Wilby, R.J.L., Leavesley, G.H., 2000. A comparison of delta change and downscaled GCM scenarios for three mountainous basins in the United States. J. Am. Water Resour. Assoc. 36, 387–397.

Hallegatte, S., Green, C., Nicholls, R.J., Corfee-Morlot, J., 2013. Future flood losses in major coastal cities. Nature Climate Change 3, 802–806. https://doi.org/10.1038/nclimate1979.

Hemer, M.A., Fan, Y., Mori, N., Semedo, A., Wang, X., 2013. Projected changes in wave climate from a multi-model ensemble. Nat. Clim. Change 3, 471–476. https://doi.org/10.1038/NCLIMATE1791.

Hersbach, H., Bell, B., Berrisford, P., Hirahara, S., Horányi, A., Muñoz-Sabater, J., Nicolas, J., Peubey, C., Radu, R., Schepers, D., Simmons, A., Soci, C., Abdalla, S., Abellan, X., Balsamo, G., Bechtold, P., Biavati, G., Bidlot, J., Bonavita, M., Chiara, G., Dahlgren, P., Dee, D., Diamantakis, M., Dragani, R., Flemming, J., Forbes, R., Fuentes, M., Geer, A., Haimberger, L., Healy, S., Hogan, R., Hólm, E., Janisková, M., Keeley, S., Laloyaux, P., Lopez, P., Lupu, C., Radnoti, G., de Rosnay, P., Rozum, I., Vamborg, F., Villaume, S., Thépaut, J., 2020. The ERA5 global reanalysis. Q. J. R. Meteorol. Soc. 2020, 1–51.

Hinkel, J., Lincke, D., Vafeidis, A.T., Perrette, M., Nicholls, R.J., Tol, R.S.J., Marzeion, B., Fettweis, X., Ionescu, C., Levermann, A., 2014. Coastal flood damage and adaptation costs under 21st century sea-level rise. Proceedings of the National Academy of Sciences of the United States of America 111 (9), 3292–3297. https://doi.org/10.1073/pnas.1222469111.

Holthuijsen, L.H., 2007. Waves in Oceanic and Coastal Waters. Cambridge, p. 387.

Horton, B. P., Khan, N. S., Cahill, N., Lee, J. S. H., Shaw, T. A., Garner, A. J., Kemp, A. C., Engelhart, S. E., Rahmstorf, S. Estimating global mean sea-level rise and its uncertainties by 2100 and 2300 from an expert survey. npj Climate and Atmospheric Science, 3, 18.

Hsiao, S.-C., Chen, H., Wu, H.-L., Chen, W.-B., Chang, C.-H., Guo, W.-D., Chen, Y.-M., Lin, L.-Y., 2020. Numerical simulation of large wave heights from super typhoon nepartak (2016) in the eastern waters of taiwan. J. Mar. Sci. Eng. 8 (3), 217. https://doi.org/10.3390/jmse8030217.

Hsiao, S.-C., Fu, H.-S., Chen, W.-B., Chang, T.-Y., Wu, H.-L., Liang, T.-Y., 2022. Assessment of future possible maximum flooding extent in the midwestern coastal region of Taiwan resulting from sea-level rise and land subsidence. Environmental Research Communications 4, 095007. https://doi.org/10.1088/2515-7620/ac8f15.

Idier, D., Bertin, X., Thompson, P., et al., 2019. Interactions between mean sea level, tide, surge, waves and flooding: mechanisms and contributions to sea level variations at the coast. Surv. Geophys. 40, 1603–1630. https://doi.org/10.1007/s10712-019-09549-5.

IPCC, 2022. In: Pörtner, H.-O., Roberts, D.C., Tignor, M., Poloczanska, E.S., Mintenbeck, K., Alegría, A., Craig, M., Langsdorf, S., Löschke, S., Möller, V., Okem, A., Rama, B. (Eds.), Climate Change 2022: Impacts, Adaptation, and Vulnerability. Contribution of Working Group II to the Sixth Assessment Report of the Intergovernmental Panel on Climate Change. Cambridge University Press, Cambridge, UK and New York, NY, USA, p. 3056. https://doi.org/10.1017/9781009325844.

Jevrejeva, S., Frederikse, T., Kopp, R.E., le Cozannet, G., Jackson, L.P., van de Wal, R.S. W., 2019. Probabilistic Sea Level Projections at the Coast by 2100. Surveys in Geophysics 40, 1673–1696.

Jones, B., O'Neill, B.C., 2016. Spatially explicit global population scenarios consistent with the Shared Socioeconomic Pathways. Environmental Research Letters 11, 084003. https://doi.org/10.1088/1748-9326/11/8/084003.

Kirezci, E., Young, I.R., Ranasinghe, R., et al., 2020. Projections of global-scale extreme sea levels and resulting episodic coastal flooding over the 21st Century. Sci. Rep. 10, 11629 https://doi.org/10.1038/s41598-020-67736-6.

Lemos, G., Semedo, A., Dobrynin, M., Behrens, A., Staneva, J., Bidlot, J.-R., Miranda, P., 2019. Mid-twenty-first century global wave climate projections: results from a dynamic CMIP5 based ensemble. Global Planet. Change 172, 69–87.

Lemos, G., Bosnic, I., Antunes, C., Vousdoukas, M., Mentaschi, L., Soares, P.M.M., 2024a. The future of the Portuguese (SW Europe) most vulnerable coastal areas under climate change – Part I: performance evaluation and shoreline evolution from a downscaled bias corrected wave climate ensemble. Ocean Eng. 302, 117661 https://doi.org/10.1016/j.oceaneng.2024.117661.

Lemos, G., Menendez, M., Semedo, A., Camus, P., Hemer, M., Dobrynin, M., Miranda, P., 2020a. On the need of bias correction methods for wave climate projections. Global Planet. Change 186, 103109.

Lemos, G., Semedo, A., Dobrynin, M., Menendez, M., Miranda, P., 2020b. Bias-corrected CMIP5-derived single-forcing future wind-wave climate projections toward the end of the twenty-first century. J. Appl. Meteorol. Climatol. 59 (9), 1393–1414. https://doi.org/10.1175/jamc-d-19-0297.1.

Lemos, G., Semedo, A., Menendez, M., Miranda, P.M.A., Hemer, M., 2021a. On the decreases in North Atlantic significant wave heights from climate projections. Clim. Dynam. https://doi.org/10.1007/s00382-021-05807-8.

Lemos, G., Semedo, A., Hemer, M., Menendez, M., Miranda, P.M.A., 2021b. Remote climate change propagation across the oceans – the directional swell signature. Environ. Res. Lett. https://doi.org/10.1088/1748-9326/ac046b.

Knutson, T., Coauthors, 2020. Tropical cyclones and climate change assessment: Part II: Projected response to anthropogenic warming. Bull. Amer. Meteor. Soc. 101, E303–E322. https://doi.org/10.1175/BAMS-D-18-0194.1.

Kulp, S.A., Strauss, B.H., 2020. New elevation data triple estimates of global vulnerability to sea-level rise and coastal flooding. Nat Commun 10, 4844. https://doi.org/10.1038/s41467-019-12808-z.

Leijala, U., Björkqvist, J.-V., Johansson, M.M., Pellikka, H., Laakso, L., Kahma, K.K., 2018. Combining probability distributions of sea level variations and wave run-up to evaluate coastal flooding risks. Nat. Hazards Earth Syst. Sci. 18, 2785–2799.

LeRoy, S.L., Pedreros, R., André, C., Paris, F., Lecacheux, S., Marche, F., Vinchon, C., 2015. Coastal flooding of urban areas by overtopping: dynamic modelling application to the Johanna storm (2008) in Gâvres (France). Nat. Hazards Earth Syst. Sci. 15, 2497–2510.

Lima, D.C.A., Lemos, G., Bento, V.A., Nogueira, M., Soares, P.M.M., 2023a. A multi-variable constrained ensemble of regional climate projections under multi-scenarios for Portugal – Part I: an overview of impacts on means and extremes. Climate Services 30. https://doi.org/10.1016/j.cliser.2023.100351, 100351.

Lima, D.C.A., Bento, V.A., Lemos, G., Nogueira, M., Soares, P.M.M., 2023b. A multi-variable constrained ensemble of regional climate projections under multi-scenarios for Portugal – Part II: sectoral climate indices. Climate Services 30, 100377. https://doi.org/10.1016/j.cliser.2023.100377.

Lin, N., Kopp, R.E., Horton, B.P., Donnelly, J.P., 2016. Hurricane Sandy's flood frequency increasing from year 1800 to 2100. Proc. Natl. Acad. Sci. USA 113, 12071–12075.

Little, C.M., et al., 2015. Joint projections of US East Coast sea level and storm surge. Nat. Clim. Change 5, 1114–1120.

Liu, C., Jia, Y., Onat, Y., Cifuentes-Lorenzen, A., Ilia, A., McCardell, G., Fake, T., O'Donnell, J., 2020. Estimating the Annual Exceedance Probability of Water Levels and Wave Heights from High Resolution Coupled Wave-Circulation Models in Long Island Sound. Journal of Marine Science and Engineering 8 (7), 475. https://doi.org/10.3390/jmse8070475.

Lopes, C.L., Alves, F.L., Dias, J.M., 2017. Flood risk assessment in a coastal lagoon under present and future scenarios: Ria de Aveiro case study. Nat. Hazards 89, 1307–1325.

Lyon, C., Saupe, E., Smith, C., Hill, D., Beckerman, A., Stringer, L., Marchant, R., McKay, J., Burke, A., O'Higgins, P., Dunhill, A., Allen, B., Riel-Salvatore, J., Aze, T., 2022. Climate change research and action must look beyond 2100. Global Change Biol. 28, 349–361.

Maraun, D., 2016. Bias correcting climate change simulations – a critical review. Curr. Clim. Change Rep. 2, 211–220.

Marcos, M., Jordà, G., Gomis, D., Pérez, B., 2011. Changes in storm surges in southern Europe from a regional model under climate change scenarios. Global Planet. Change 77, 116–128.

Marcy, D., Brooks, W., Draganov, K., Hadley, B., Haynes, C., Herold, N., McCombs, J., Pendleton, M., Schmid, K., Sutherland, M., et al., 2011. New mapping tool and techniques for visualizing sea level rise and coastal flooding impacts. In: Proceedings of the 2011 Solutions to Coastal Disasters Conference. Anchorage, AK, USA, pp. 474–490. https://doi.org/10.1061/41185(417)42, 26–29 June 2011.

Melet, A., Buontempo, C., Mattiuzzi, M., Salamon, P., Bahurel, P., Breyiannis, G., Burgess, S., Crosnier, L., Le Traon, P.-Y., Mentaschi, L., Nicolas, J., Solari, L., Vamborg, F., Voukouvalas, E., 2021. European copernicus services to inform on sea-level rise adaptation: current status and perspectives. Front. Mar. Sci. 8, 703425.

Mentaschi, L., Vousdoukas, M.I., Voukouvalas, E., Dosio, A., Feyen, L., 2017. Global changes of extreme coastal wave energy fluxes triggered by intensified teleconnection patterns. Geophys. Res. Lett. 44, 2416–2426. https://doi.org/10.1002/2016GL072488.

Morim, J., Hemer, M.A., Cartwright, N., Strauss, D., Andutta, F., 2018. On the concordance of 21st century wind-wave climate projections. Global Planet. Change 167, 160–171.
Morim, J., Hemer, M.A., Wang, X., Cartwright, N., Trenham, C., Semedo, A., Young, I., Bricheno, L., Camus, P., Casas-Prat, M., Erikson, L., Mentaschi, L., Mori, N., Shimura, T., Timmermans, B., Aarnes, O., Breivik, Ø., Behrens, A., Dobrynin, M., Menendez, M., Staneva, J., Wehner, M., Wolf, J., Kamranzad, B., Webb, A., Stopa, J., Andutta, F., 2019. Robustness and uncertainties in global multivariate wind-wave climate projections. Nat. Clim. Change 9, 711–718.
Nahon, A., Fortunato, A.B., Oliveira, F.S.B.F., Azevedo, A., Henriques, M.J., Silva, P.A., Baptista, P., Freire, P., 2023. 2DH modelling and mapping of surfbeat-driven flooding in the shadow of a jettied tidal inlet. Coast Eng. 184, 104342.
Nunes, A.J., Cordeiro, M.F.N., 2013. Alteração da linha de costa entre a Figueira da Foz e S. Pedro de Moel após o prolongamento do molhe norte do Mondego. Actas do VI Congresso Nacional de Geomorfologia, Coimbra, pp. 6–10.
Oliveira, F.S.B.F., Brito, F.A., 2015. Evolução da morfologia costeira a sul da embocadura do rio Mondego, de 1975 a 2011. In: VIII Congresso sobre Planeamento e Gestão das Zonas Costeiras dos Países de Expressão Portuguesa. Universidade de Aveiro, Aveiro, p. 15.
Parker, K., Erikson, L., Thomas, J., et al., 2023. Relative contributions of water-level components to extreme water levels along the US Southeast Atlantic Coast from a regional-scale water-level hindcast. Nat Hazards 117, 2219–2248. https://doi.org/10.1007/s11069-023-05939-6.
Parkinson, RW, Ogurcak, DE, 2018. Beach nourishment is not a sustainable strategy to mitigate climate change. Estuar Coast Shelf Sci 212, 203–209. https://doi.org/10.1016/j.ecss.2018.07.011.
Peduzzi, P., et al., 2012. Global trends in tropical cyclone risk. Nat. Clim. Change 2, 289–294.
Pinto, C.A., 2016. Coastal erosion and sediment management in Portugal. In: Proceedings of the CEDA Iberian Conference—Dredging for Sustainable Port Development, Lisbon, Portugal.
Pinto, C.A., Silveira, T.M., Taborda, R., 2015. Alimentação artificial das praias da Costa da Caparica: síntese dos resultados de monitorização (2007 a 2014). In: 3ª Conferencia sobre morfodinâmica estuarina e costeira. Universidade do Algarve, 14-15 May 2015. Faro.
Pinto, C.A., Silveira, T.M., Teixeira, S.B., 2020. Beach nourishment practice in mainland Portugal (1950–2017): overview and retrospective. Ocean Coast Manag. 192, 105211.
Pinto, C.A., Taborda, R., Andrade, C., 2007. Evolução recente da linha de costa no troço Cova do Vapor – S. João da Caparica. In: 5as Jornadas Portuguesas de Engenharia Costeira e Portuária, Lisboa. PIANC. AIPCN, Lisboa, p. 13.
Pinto, C., Taborda, R., Andrade, C., Baptista, P., Silva, P., Alves, Mendes, D., Pais-Barbosa, J., 2022. Morphological development and behaviour of a shoreface nourishment in the Portuguese western coast. J. Mar. Sci. Eng. 10 (2), 146. https://doi.org/10.3390/jmse10020146.
Ponte Lira, C., Nobre Silva, A., Taborda, R., Freire de Andrade, C., 2016. Coastline evolution of Portuguese low-lying sandy coast in the last 50 years: an integrated approach. Earth System Science Data 8 (1), 265–278. https://doi.org/10.5194/essd-8-265-2016.
Priestley, M.D.K., Catto, J.L., 2022. Future changes in the extratropical storm tracks and cyclone intensity, wind speed, and structure. Weather Clim. Dynam. 3, 337–360. https://doi.org/10.5194/wcd-3-337-2022.
Pugh, D., Woodworth, P.L., Woodworth, P., 2014. Sea-Level Science: Understanding Tides, Surges, Tsunamis and Mean Sea-Level Changes, 2014. Cambridge University Press, p. 395. https://doi.org/10.1017/CBO9781139235778, 1107028191, 9781107028197.
Ranasinghe, R., 2016. Assessing climate change impacts on open sandy coasts: A review. Earth-Science Reviews 160, 320–332. https://doi.org/10.1016/j.earscirev.2016.07.011.
Rasmussen, D.J., et al., 2018. Extreme sea level implications of 1.5 °C, 2.0 °C, and 2.5 °C temperature stabilization targets in the 21st and 22nd century. Environ. Res. Lett. 13, 034040.
Riahi, K., Rao, S., Krey, V., Cho, C., Chirkov, V., Fischer, G., Kindermann, G., Nakicenovic, N., Rafaj, P., 2011. Rcp 8.5 – a scenario of comparatively high greenhouse gas emissions. Climatic Change 109, 33–57. https://doi.org/10.1007/s10584-011-0149-y.
Ribeiro, A.S., Lopes, C.L., Sousa, M.C., Gomez-Gesteira, M., Dias, J.M., 2021. Flooding conditions at Aveiro port (Portugal) within the framework of projected climate change. J. Mar. Sci. Eng. 9, 595. https://doi.org/10.3390/jmse9060595.
Rocha, C., Antunes, C., Catita, C., 2020. Coastal vulnerability assessment due to sea level rise: the case study of the atlantic coast of mainland Portugal. Water 12 (2), 360. https://doi.org/10.3390/w12020360.
Rocheta, E., Evans, J., Sharma, A., 2017. Can bias correction of regional climate model lateral boundary conditions improve low-frequency rainfall variability? J. Clim. 30, 9785–9806.
Roelvink, J.A., Van Banning, G.K.F.M., 1994. In: Verwey, A., Minns, A.W., Babovic, V., Maksimovic, C. (Eds.), *Hydroinformatics*: Design and Development of DELFT3D and Application to Coastal Morphodynamics. Balkema, Rotterdam, The Netherlands, pp. 451–456.
Roelvink, J.A., Reniers, A., van Dongeren, A., van Thiel de Vries, J., McCall, R., Lescinski, J., 2009. Modeling storm impacts on beaches, dunes and barrier islands. Coast Eng. 56, 1133–1152.
Santos, F.D., Mota Lopes, A., Moniz, G., Ramos, L., Taborda, R., 2014. In: Santos, Filipe Duarte, Penha-Lopes e, Gil, Lopes, António Mota (Eds.), Grupo de Trabalho do Litoral: Gestão da Zona Costeira: O desafo da mudança. Lisboa (ISBN: 978-989-99962-1-2).
Rosati, J.D., Dean, R.G., Walton, T.L., 2013. The modified Bruun Rule extended for landward transport. Marine Geology 340, 71–81.
Santos, J.F.C., 2020. Custos e benefícios de mitigar a erosão costeira no litoral de Ovar. Master's thesis. Universidade de Aveiro, Departamento de Engenharia Civil, p. 157.
Sayol, J.M., Marcos, M., 2018. Assessing Flood Risk Under Sea Level Rise and Extreme Sea Levels Scenarios: Application to the Ebro Delta (Spain). Journal of Geophysical Research: Oceans 123 (2), 794–811. https://doi.org/10.1002/2017JC013355.
Schubert, J.E., Sanders, B.F., 2012. Building treatments for urban flood inundation models and implications for predictive skill and modeling efficiency. Adv. Water Resour. 41, 49–64.
Semedo, A., Behrens, R., Sterl, A., Bengtsson, L., Günther, H., 2013. Projection of global wave climate change toward the end of the twenty-first century. J. Clim. 26, 8269–8288.
Senechal, N., Coco, G., Bryan, K.R., Holman, R.A., 2011. Wave run-up during extreme storm conditions. J. Geophys. Res.: Oceans 116 (C7).
Soares, P.M.M., Careto, J.A.M., Cardoso, R.M., Goergen, K., Katragkou, E., Sobolowski, S., Coppola, E., Ban, N., Belušić, D., Berthou, S., Caillaud, C., Dobler, A., Hodnebrog, Ø., Kartsios, S., Lenderink, G., Lorenz, T., Milovac, J., Feldmann, H., Pichelli, E., Truhetz, H., Demory, M.E., de Vries, H., Warrach-Sagi, K., Keuler, K., Raffa, M., Tölle, M., Sieck, K., Bastin, S., 2022. The added value of km-scale simulations to describe temperature over complex orography: the CORDEX FPS-Convection multi-model ensemble runs over the Alps. Clim. Dynam. https://doi.org/10.1007/s00382-022-06593-7.
Soares, P.M.M., Careto, J.A.M., Russo, A., Lima, D.C.A., 2023b. The future of Iberian droughts: a deeper analysis based on multi-scenario and a multi-model ensemble approach. Nat. Hazards 117, 2001–2028. https://doi.org/10.1007/s11069-023-05938-7.
Soares, P.M.M., Lemos, G., Lima, D.C.A., 2023a. Critical analysis of CMIPs Past Climate Model Projections in a regional context: the Iberian climate. International Journal of Climatology. https://doi.org/10.1002/joc.7973.
Soares, P.M.M., Lima, D.C.A., 2022. Water scarcity down to earth surface in a Mediterranean climate: the extreme future of soil moisture in Portugal. J. Hydrol. 615, 128731 https://doi.org/10.1016/j.jhydrol.2022.128731.
Storlazzi, C., Gingerich, S.B., Dongeren, A., Cheriton, O., Swarzenski, P., Quataert, E., Voss, C., Field, D., Annamalai, H., Piniak, G., McCall, R., 2018. Most atolls will be uninhabitable by the mid-21st century because of sea-level rise exacerbating wave-driven flooding. Sci. Adv. 4 (4) https://doi.org/10.1126/sciadv.aap9741.
Tebaldi, C., Ranasinghe, R., Vousdoukas, M., Rasmussen, D.J., Vega-Westhoff, B., Kirezci, E., Kopp, R.E., Sriver, R., Mentaschi, L., 2023. Extreme sea levels at different global warming levels. Nat. Clim. Change 1, 746–751.
Toimil, A., Losada, I.J., Camus, P., Díaz-Simal, P., 2017. Managing coastal erosion under climate change at the regional scale. Coastal Enfineering 128, 106–122. https://doi.org/10.1016/j.coastaleng.2017.08.004.
Toimil, A., Camus, P., Losada, I.J., Le-Cozannet, G., Nicholls, R.J., Idier, D., Maspataud, A., 2020. Climate change-driven coastal erosion modelling in temperate sandy beaches: methods and uncertainty treatment. Earth Sci. Rev. 202, 103110 https://doi.org/10.1016/j.earscirev.2020.103110.
Temmerman, S., Meire, P., Bouma, T., et al., 2013. Ecosystem-based coastal defence in the face of global change. Nature 504, 79–83. https://doi.org/10.1038/nature12859.
Thompson, C.M., Frazier, T.G., 2014. Deterministic and probabilistic flood modeling for contemporary and future coastal and inland precipitation inundation. Applied Geography 50, 1–14.
Toimil, A., Camus, P., Losada, I.J., Alvarez-Cuesta, M., 2021. Visualising the uncertainty cascade in multi-ensemble probabilistic coastal erosion projections. Front. Mar. Sci. 8, 683535 https://doi.org/10.3389/fmars.2021.683535.
Tolman, H.L., 2002. User Manual and System Documentation of WAVEWATCH-III Version 2.22. *Tech. Report 222*. NOAA/NWS/NCEP/MMAB.
Vieira, R., Antunes, C., Taborda, R., 2012. Caracterização da sobreelevação meteorológica em Cascais nos últimos 50 anos. In: Proceedings of 2as Jornadas de Engenharia Hidrográfica, Lisbon, Portugal, 21–22 June 2012, pp. 21–24, 978-989-705-035-0.
Vitousek, S., et al., 2017. Doubling of coastal flooding frequency within decades due to sea-level rise. Sci. Rep. 7, 1399.
Vousdoukas, M.I., Mentaschi, L., Voukouvalas, E., Verlaan, M., Feyen, L., 2017. Extreme sea levels on the rise along Europe's coasts. Earth's Future 5 (3), 304–323.
Vousdoukas, M.I., Mentaschi, L., Voukouvalas, E., et al., 2018. Global probabilistic projections of extreme sea levels show intensification of coastal flood hazard. Nat. Commun. 9, 2360. https://doi.org/10.1038/s41467-018-04692-w.
Vousdoukas, M.I., Ranasinghe, R., Mentaschi, L., Plomaritis, T.A., Athanasiou, P., Luijendijk, A., Feyen, L., 2020. Sandy coastlines under threat of erosion. Nat. Clim. Chang. 10, 260–263. https://doi.org/10.1038/s41558-020-0697-0.
Vousdoukas, M.I., Voukouvalas, E., Annunziato, A., Giardino, A., Feyen, L., 2016. Projections of extreme storm surge levels along Europe. Clim. Dynam. 47 (9), 3171–3190. https://doi.org/10.1007/s00382-016-3019-5.
Wahl, T., Chambers, D.P., 2015. Evidence for multidecadal variability in US extreme sea level records. J. Geophys. Res.: Oceans 120, 1527–1544. https://doi.org/10.1002/2014JC010443.
Wahl, T., et al., 2017. Understanding extreme sea levels for broad-scale coastal impact and adaptation analysis. Nat. Commun. 8, 16075.
Woodruff, J.D., Irish, J.L., Camargo, S.J., 2013. Coastal flooding by tropical cyclones and sea-level rise. Nature 504, 44.
Van Loon-Steensma, J. M., Vellinga, P. 2019. "How "wide green dikes" were reintroduced in The Netherlands: a case study of the uptake of an innovative measure in long-term strategic delta planning," Journal of Environmental Planning and Management, Taylor & Francis Journals, vol. 62(9), pages 1525-1544, July.